MACHINING PROCESSES OF SAPPHIRE: AN OVERVIEW

Pravin Pawar[1], Raj Ballav [2], Amaresh Kumar [3]

[1,2,3]Department of Manufacturing Engineering, National Institute of Techonlogy, Jamshedpur, 831014, Jharkhand, India.

Corresponding author: Pravin Pawar, E-mail: pravin.1900@gmail.com

Abstract: Sapphire is a single crystal form of α-alumina. It has a number of chemical, mechanical, electrical, optical and biomedical properties due to which it is applicable in the field of industrial, electrical and electronics, optical, defense and medical. The hardness and brittleness make sapphire machining very difficult and costly. This paper includes a brief review of seven machining processes used for sapphire material. The last 30 years research work of sapphire material has been scrutinized and presented in tabulated form with the specific focus on the input parameters and achieved results in each process. From this review, it is observed that the laser machining process, grinding process, polishing process are mostly applied on the sapphire material, while EDM is less used process or it can be an area for future research. This survey will be a database for new findings in sapphire as it provides quick referencing on machining processes. Also helpful for selecting proper, economic and effective machining process which will provide specific output parameters.
Key words: Sapphire, Laser Machining Process, Grinding Process, Polishing Process, Compound Process.

1. INTRODUCTION

In recent years, the manufacturing processes giving their attention on improvement in productivity rates, reduction in production costs with the good quality product [1]. Machining is a manufacturing method, which makes changes in shape, dimensions and surface finish to obtain a high-quality product [2]. The ceramics and composites materials can be machined by using a combination of advanced trends in manufacturing processes to obtain a high-quality product having lowest cost [3]. In engineering field the use of a hard material is very expensive is due to its low strength of cutting tools which caused low productivity rate [4]. Hence, next to diamond the sapphire is one of those hardest materials having 9 Mohs hardness. The Auguste Verneuil (1891) firstly developed and produced the large sapphire crystals having high-melting point on an industrial scale by using an artificial method, which in 1902 converted into commercial method [5-7]. The Sapphire is also called as corundum which is a natural crystal of α-aluminum oxide having trigonal symmetry. The pure corundum crystals are colorless and known as leucosapphire. Now a day, these colorless corundum crystals commonly known as “sapphire” which is also termed as blue corundum in historical periods. It is stable up to 2050ºC melting temperature [6, 8, 9].

Sapphire is one of the ceramic material. It is a single crystal form of α-alumina, which contains a number of chemical, mechanical, electrical, optical and biomedical properties. The chemical properties include chemical resistance, chemical compatibility, chemical stability and high anti-corrosion. The high abrasion resistance, high hardness, shock resistance, high thermal stability, high strength, high pressure, abrasion resistant, high temperature, rapid heating and cooling, high rigidity, high elastic modulus, brittleness, wear resistance are the mechanical properties of sapphire. Whereas, the electrical and optical properties are the high optical transmission, optical transparency, good electric insulation and low dielectric loss. It also exhibits biomedical properties such as biocompatibility, cell adhesion and proliferation behavior [6-20, 23-31, 33, 35, 37-54, 56-59, 61, 63-75, 77-85, 87, 88-91, 93-96].

Due to these wide ranges of properties sapphire material has widely used in different fields. In industrial fields it is used in jewel bearings for precision mechanical instruments, ultracentrifuge cell windows, corrosion-resistant cells, crucibles, tubes, semiconductor wafer carrier plates, high-temperature process windows, TV receivers, mobile phones, household appliances, jewelry industry, measuring glasses, reactor housings, watch bearing, microreactors, high temperature or high-pressure cells. The electrical and electronics areas sapphire material utilized in Liquid Crystal Display television sets (LED-LCD TVs), bar code scanners, blue light-emitting diodes, diode lasers, transparent electronic substrates, cooling of electronic devices, optoelectronic, semiconductor devices, sensors, infrared detectors and superconductor, photoelectronic, microelectronic, read/write laser sources, IC chips. The optical field shows sapphire applicability such as in lamps and lamp envelopes, optical windows, scratch-proof crystal face of expensive wrist watches, sodium lamp tubes, high-pressure cell optics, high-power laser optics, optical

flats, microwave output windows, watch glass, sapphire lenses and prisms, violet/blue/green light emitting diodes and photodetectors, laser diodes, solid lasers, optical fibers, storage on magnetic and optical medias. The sapphire material is also used in advanced medical field for making sapphire tubes, plates, spectroscopy, chemical and biological analysis, ultraviolet sterilizations, medical equipment, inserted (implanted) in human tissue, sapphire tools, endoscopes (tips of different shapes), laser surgical apparatuses, IR-scalpels, microfluidics, cutting blades, surgical tips, biomedical equipment, beam delivery for medical applications. The GaN light emitting diodes, missile domes, and transparent armor are the aerospace and military application in which sapphire is employed [6-31, 33, 35-54, 56-58, 62-75, 77-85, 88-90, 92-96].

M. Klejch et al. [10] created single-crystal sapphire filaments by applying the edge-defined film-fed growth technique. E. Dobrovinskaya et al. [11] have deeply studied and explained properties, manufacturing methods and various applications of sapphire. Z. Li et al. [12] first time reviewed various machining processes for sapphire wafer in the year 2011. Similarly, P. Pawar et al. [13, 14] surveyed literature of various machining processes used for alumina and alumina composites ceramic materials. Y. Zhang et al. [15] studied literature review on chemical mechanical polishing of sapphire material. V. Rogov [16] reviewed physicochemical processes for the formation of sapphire functional surfaces with special reference to the polishing processes. D. Wen et al. [17] explained the surface integrity of sapphire wafer by using abrasive machining processes such as grinding, lapping and polishing processes.

Sapphire is very hard and brittle material which causes limitations during machining but besides this, it exhibits various applications. Hence, to eliminate its limitations lots of research work was carried out on sapphire with special reference to machining process along with the experimental and theoretical study. Thus to take an overview of past to present research work on sapphire material this investigation has been undertaken which will useful for further research on this material.

2. MACHINING PROCESSES OF SAPPHIRE

There are different types of machining process used for sapphire material. The fig. 1 shows a graphical representation of sapphire machining processes i.e. laser machining process, grinding process, polishing process, lapping process, new developed machining process, compound machining process and electro discharge machining process.

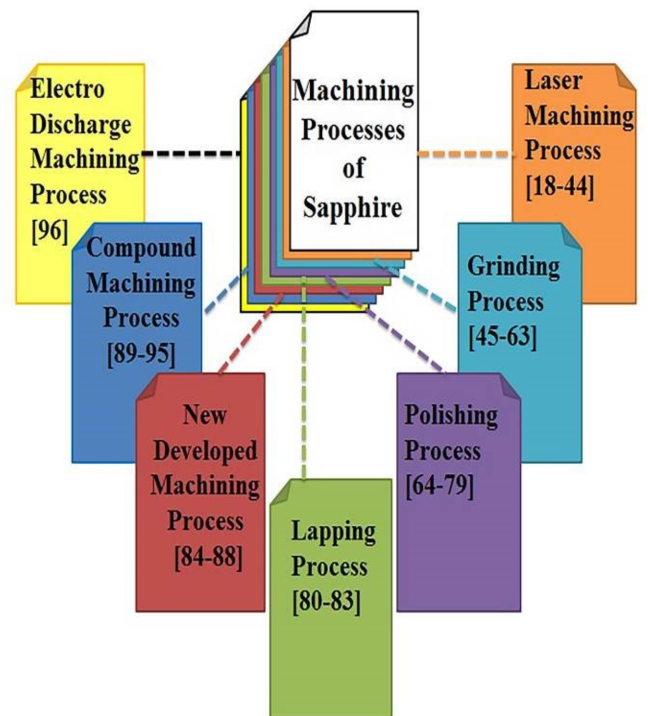

Fig.1. Machining processes of sapphire material

2.1 Laser Machining Process

Laser beam machining is a non-conventional process which is based on principles of quantum theory. The laser is an extreme source of light having extraordinary properties. When a laser is focused to the workpiece the machining of material take place. The unique properties of the laser is its light waves travel up to very long distances with a very little deviation and the energy of coherent photons or laser beam converted into thermal energy. Due to this thermal energy workpiece surface undergo to the heating and melting or vaporizing processes [18-44]. The process is based on different types of lasers used for sapphire machining i.e. Ti:Sapphire laser, Nd: YAG laser, Solid State laser, fiber laser, ultraviolet laser, Yb:KYW laser, ytterbium laser, F_2 Laser, Krf-Excimer, XeCl excimer laser, copper vapour laser, Fluorine laser.

a. Ti:Sapphire Laser

The figure 2 shows amplified Ti:Sapphire laser system which provides high-intensity laser pulses with a maximum pulse energy and repetition rate having a central wavelength. The Ti:sapphire produces femtosecond pulsed laser. The thin film attenuation filters was used to adjust the average femtosecond laser output power. Also the lenses of different focal lengths used to focus laser beams on the sapphire material and material gets irradiated through an aperture situated normal to the sapphire. [18-24].

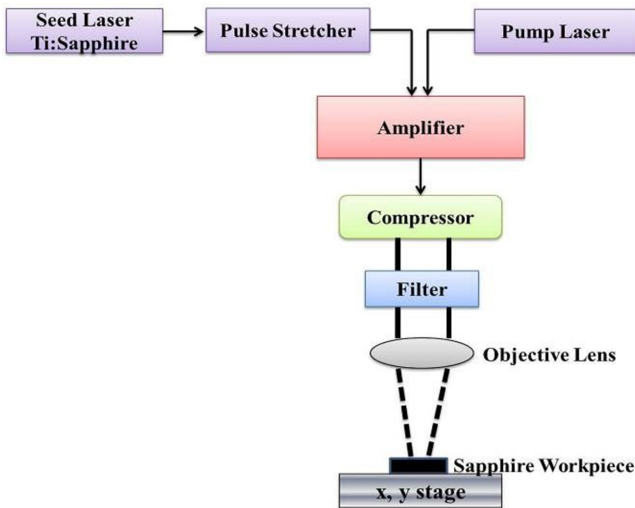

Fig. 2. Schematic diagram of the Ti:Sapphire laser (Redrawn from [23])

A. Shamir et al. [18] achieved uniform ablation and 1mm×15mm deep area of the sapphire substrate by using femtosecond pulses laser process. They observed scan speed has a minor effect on ablation depth; whereas, the large scan speeds reduce the uniformity of ablated surface. Therefore, the deepest and uniform ablation achieved at low scan speeds with a pattern of snake-like ablation. L. Qi et al. [19] experimented on sapphire by using laser irradiation process. The two ablation phases were observed in single laser pulse irradiation. In the case of multiple laser pulse irradiation, craters without cracks were achieved. However, as the number of laser pulses increases simultaneously the increase in depth of craters observed. X. Wang et al. [20] investigated micromachining of sapphire using femtosecond pulse laser process with ambient air medium. The results showed that the surface ablation threshold gets decreased notably by increasing the pulse number applied to the surface. The process produced submicrometer pit holes of dimension smaller than 1mm with a high quality machined surface. H. Zheng et al. [21] discussed recent research work in femtosecond laser, by which the nano/micro structures were created on compound semiconductors. They irradiated surfaces of InP and GaN/sapphire by applying femtosecond laser pulses which resulted into structures of wavelength and sub-wavelength periodic surface. They observed that, the periodic structure morphology was dependent on number of laser pulses and laser beam polarization. Whereas, the period was based on incident laser fluence. K. Kim et al. [22] achieved results i.e. smooth and clean features with high rate of ablation in sapphire by using femtosecond laser micromachining of sapphire which proven that this process is suitable for the micro-scale machining of important material. G. Rice et al. [23] observed that 800nm femtosecond laser ablation of sapphire is superior to 355nm nanosecond laser machining process. According to them, the grooves depth increased directly by the number of scans. The femtosecond laser machining process can create smooth and clean features having high ablation rates on important materials. K. Yin et al. [24] proposed a method for the manufacturing of line patterned superwetting surface on sapphire material by applying femtosecond laser process. They observed that, when the sizable microgrooves nanostructures occurred that time wettability increases significantly. This study has excellent potential to enhance the performance of heat pipes in the substrate of electronic devices.

b. Nd:YAG Laser

The Nd:YAG laser system is shown in figure 3. The Nd:YAG laser and Q-switched with an acousto-optic Q-switch are composed in the oscillator. By adujusting the incident angle of laer beam, the shape of scribing was controlled. It also controls the focal spot size and focused through the F-theta lens. The F-theta lens contains two sets of mirror which are mounted on galvanometer. The galvanometer was used to compensate the optical distortion in F-theta lens. Besides the F-theta lens, the CCD camera was mounted which was used to observed the position of sapphire wafer. The metal plate was placed to the focal plane. Wheras, on the plate surface a sapphire was adjusted. The laser beam focuses on the surface of metal plate passing through F-theta lens and sapphire wafer which was resulted into removal of material. [25-32].

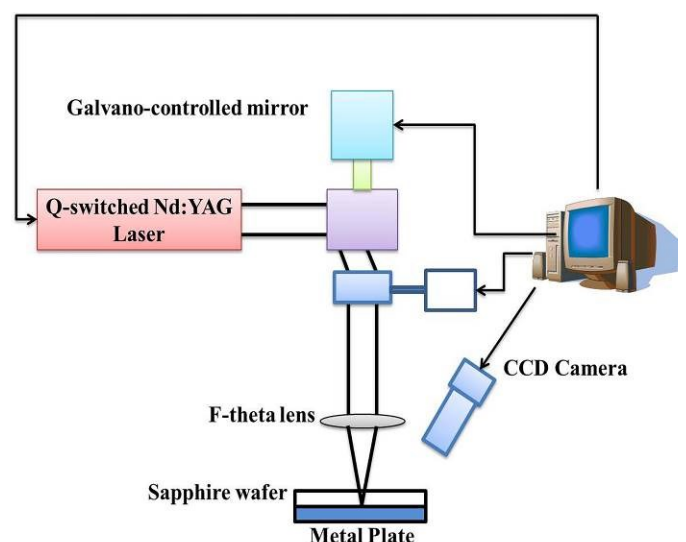

Fig. 3. Schematic diagram of the Nd:YAG laser (Redrawn from [28])

T. Chen et al. [25] obtained ablation on sapphire material by using a near-ultraviolet nanosecond pulsed Nd:YAG laser machining process. They concluded that the surface quality and efficiency of laser micromachining are dependent on focus length, pulse repetition rate, and the beam feed rate. T. Chen et al. [26] investigated the ablation rates and laser micromachining of sapphire material by using near UV and mid-UV nanosecond pulsed Nd:YAG lasers process. The 266nm laser offers high pulsed energy normalized ablation rates to the sapphire material because it is a finite absorption material having a high melting temperature. According to them, the laser ablation process is more photochemical which decreases the localized heating shock effects. J. Han et al. [27] observed that the depth of keyhole is almost directly proportional to laser pulse energy in 1064nm Nd:YAG pulsed laser process. J. Lee et al. [28] scrubbed and cut a sapphire wafer by metal surface plasma using Q-switched Nd:YAG laser having 5W power. This method can successfully separate blue LED devices which grown on Saphire wafer. J. Lee et al. [29] scrubbed and cut blue LED wafer by applying laser induced plasma assisted ablation (LIPPA) method with a q-switched Nd:YAG laser. H. Horisawa et al. [30] reduced the thermal influences observed during laser machining of sapphire by investigating the short-pulse ultraviolet laser effects. For this study, they used Fifth HG wave of Nd:YAG laser (213nm). They controlled material removal rate and achieved a smooth surface having smaller roughness. D. Wyszynski et al. [31] developed a mathematical model for the precise laser cutting of Al_2O_3 crystals. From the results, it was observed that, this model gives rough information about improvement in efficiency and accuracy of machining process. A. Tam et al. [32] etched on single crystal sapphire using a picosecond laser beam at 266nm wavelength. They observed that picosecond laser can produce better surface quality without material damage or extensive debris deposition.

c. Solid State Laser

The solid state laser system presented in figure 4. It offers a high pulse repetition rates and pulse energies to the machined sapphire. In this process the solid state laser beam transmitted through mirrors and then gets expanded by the beam expansion telescope. After that with the help of focal lens this expanded beam was focused on the sapphire wafer to remove the expected material. [33, 34]. A. Tamhankar et al. [33] concluded that, the 355nm *Q*-switched diode-pumped solid-state laser process is significant for obtaining LED sapphire scribing. The short pulse widths at optimal low fluence regime and high repetition rates are most suitable conditions for this process. A. Nebel et al. [34] formed ablation depth on sapphire material by using novel solid-state picosecond lasers which give high efficiency, high average power and high repetition rates. As well as the advanced modulators having digital timing control gives new potential to this process because they generate a sequence of pulses which support the high ablation rates. The surface without micro-cracks, nominal debris and damage free adjacent structures was achieved by using this process.

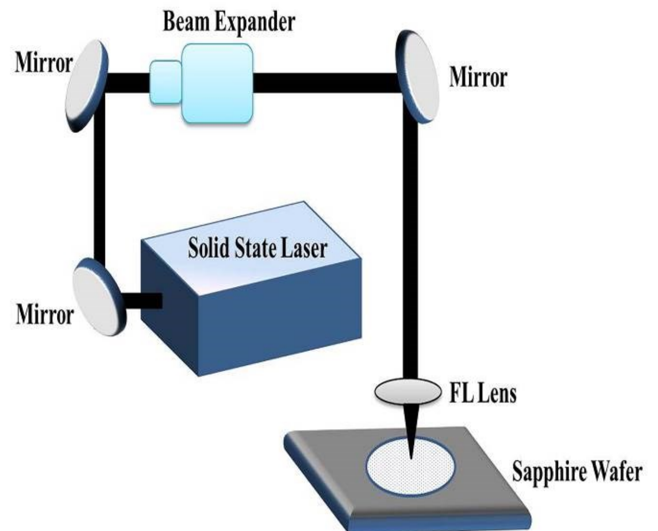

Fig. 4. Schematic diagram of the solid state laser (Redrawn from [33])

d. Fiber Laser

The pulsed fiber chirped amplifier laser with a central wavelength produces a variable repetition rate and variable full pulse duration. The laser beam was expanded through a beam expander and then transferred and focused on sapphire substrate with the help of a scan head. The laser, scan head and motion controller were operated by using the computer. The experimental setup for fiber laser is shown in figure 5.

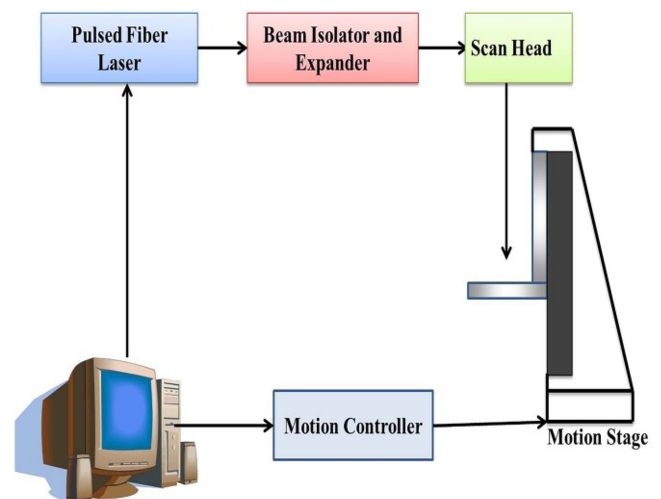

Fig. 5. Schematic diagram of the fiber laser (Redrawn from [35])

[35, 36]. Y. Zhou et al. [35] achieved 3 to 80 times greater ablation rate on sapphire by using laser-induced backside ablation with nanosecond lasers. It produces good ablation quality in which backing layer don't have any chemical contamination.They observed that this ablation rate was not influenced by the laser pulse duration. D. Wortmann et al. [36] manufactured microchannels and nanostructures of sapphire by using femtosecond laser irradiation with chemical etching having HF acid in aqueous solution form. The obtained hollow nanoplanes were elliptical in shape, up to 1mm feature length with high aspect ratio. They suggested that this process can be useful for manufacturing of microfluidic devices which are useful in the scientific field.

e. Ultraviolet Laser

The ultraviolet laser source, optical system, and work table were controlled by a computer. The Laser beam was transferred into the optical system and focused by f-theta focusing lens on the sapphire surface due to which the sapphire surface was ablated and represented in figure 6. X. Wei et al. used a Q-switched 355nm ultraviolet laser with nanosecond pulses for the polishing of the sapphire substrate. They obtained smaller interaction angle with lower surface roughness. According to them for precision polishing the ultraviolet laser polishing is the most suitable process [37].

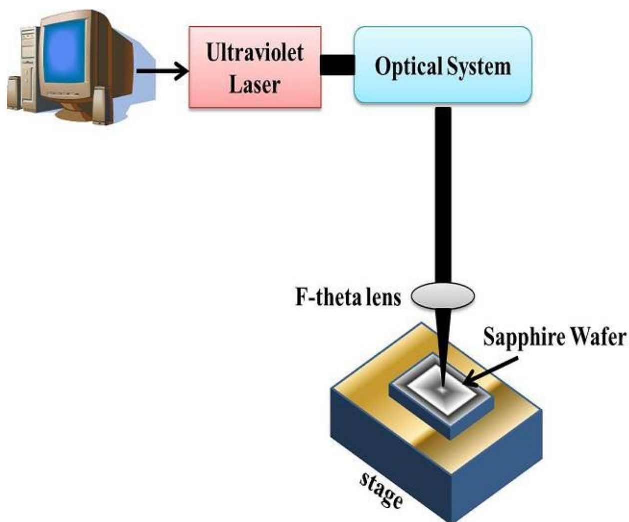

Fig. 6. Schematic diagram of the ultraviolet laser (Redrawn from [37])

f.Yb:KYW Laser

He Yb:KYW laser system is shown in figure 7. TThe Yb:KYW chirped-pulse-regenerative amplification laser system produced the laser beam which was focused perpendicularly to the sapphire surface by using a numerical aperture microscope objective. The stationary laser beam at constant scanning speed was controlled by using a computer at linear stage [38].

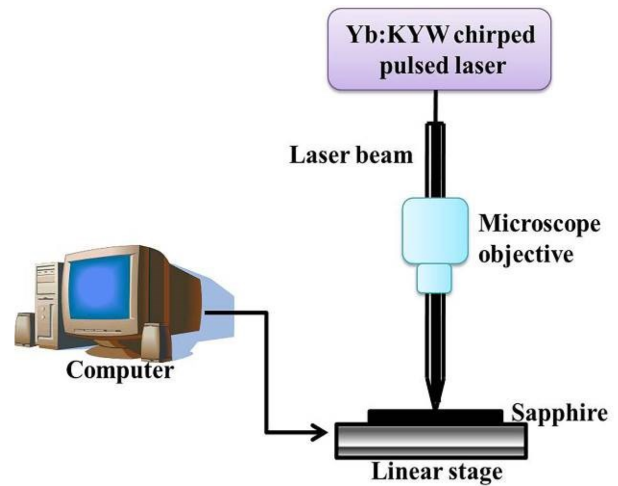

Fig. 7. Schematic diagram of the Yb:KYW laser

R. Vilar et al. cut single-crystal sapphire parallel to the planes using a femtosecond laser radiation process with considerably larger intensity than the ablation threshold. They found that at higher fluencies conditions the more disrupting and expansive fracture, exfoliation and removal of ablation debris were observed during laser cutting operation [38].

g. Ytterbium Laser

The ytterbium femtosecond laser irradiation process used for the sapphire surface micron-resolution patterning. The laser beam transmitted through the optical lens group which includes wave plate, polarizing beam spitter and iris. This optical lens group helps to reduce the Gaussion laser beam. Then the transmitted laser beam passed through a dicroic mirror which was monitored by charge-coupled-device. Then the beam was focused on sapphire by passing through objective lens and resulted into material irradiation. The schematic diagram for ytterbium laser system is shown in figure 8 [39].

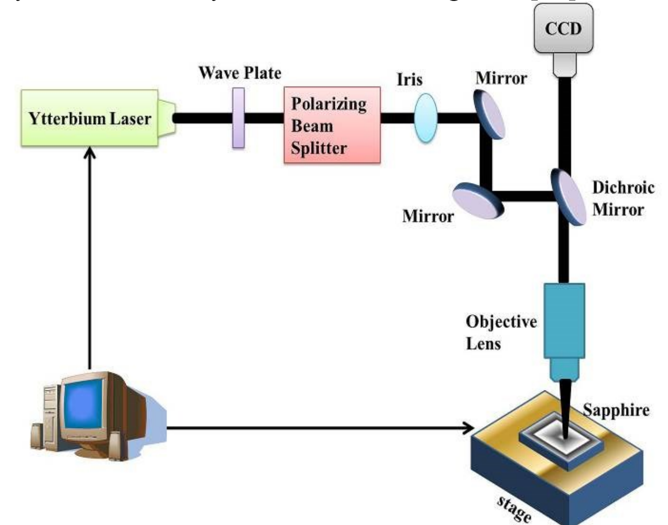

Fig. 8. Schematic diagram of the ytterbium laser (Redrawn from [39])

C. Chang et al. fabricated sapphire surface having two dimensional array patterns. According to them, this process will play a significant role in light extraction and micro-optical application [39].

h. F_2 Laser

In this process the laser beam was passed through the refractive optical elements system which was flushed by nitrogen to get the high optical transmission. The F_2 laser beam was delivered through the system and then transmitted through the insertable mirror to dielectric mirror which was monitored by CCD and oprical coherence tomography (OCT). The OCT module inclides Michelson interferometer and galvanometric scanner system which provides alighnment and focus control to the laser beam. After that the bram was passes through the filed lens mask and Schwarzschild lens which was worked as refractive object and the ablation of sapphire material was carried out and represented in figure 9. M. Wiesner et al. used F_2 lasers ablation operating at 157nm for the fabrication of sapphire materials which resulted in crack free surface having grating patterns of 1 μm period. According to them, by using this process the micro-optical elements can be successfully fabricated [40].

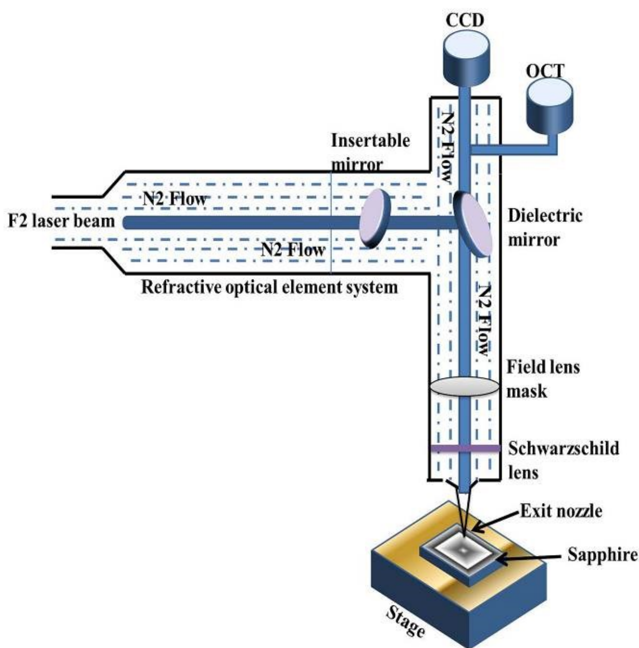

Fig. 9. Schematic diagram of the F_2 Laser (Redrawn from [40])

i. Krf-Excimer Laser

This process includes etching chamber which contains liquid absorber. This liquid was a different concentration of pyrene, acetone, tetrachoroethylene or cyclohexane. On the top of this chamber 2 inch transparent sample was fixed. Then the laser beam projected through the objective as well as transmitted by this transparent sample and gets absorbed at its backside by liquid absorber which resulted into the etching of sapphire material. The figure 10 presents experimental setup of KrF eximer laser system [41].

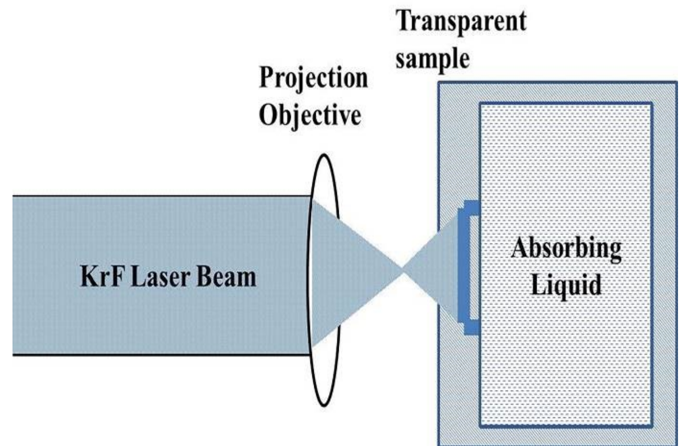

Fig. 10. Schematic diagram of the Krf-Excimer (Redrawn from [41])

R. Bohme et al. manufactured well defined three dimensional microstructures with low surface using KrF-excimer laser etching process. According to observations, the etch threshold fluence and etch rates are dependent on liquid solvent and dissolved pyrene concentration. They observed precision machining with no debris formation during this process [41].

j. XeCl excimer Laser

The experimental setup for XeCl setup is shown in figure 11. This process is also contains same experiemental set up as above. Besides this, the one side of sapphire was in contact with pyrene in acetone having a concentration of 0.4 M etchant solution, whereas other side was irradiated by XeCl excimer laser. The diffractive gray tone phase mask was utilized to control the intensity of a XeCl excimer laser.

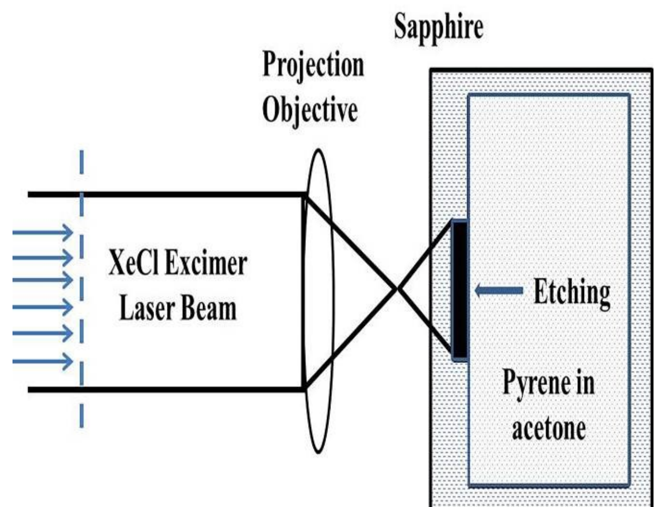

Fig. 11. Schematic diagram of the XeCl excimer Laser (Redrawn from [42])

G. Kopitkovas et al. used laser wet etching technique for the study of UV transparent dielectric material. They obtained 10nm to 3µm etched features roughness which was based on laser fluence and the material. According to them this is the most suitable process for the fast microstructuring of UV transparent dielectric materials. They also observed that the roughness achieved from this process can be varied from 5nm to some micrometers [42].

k. Copper Vapour Laser

The figure 12 shows experimental procedure of copper vapour laser. The UV copper vapour laser system provides better beam pointing stability and power stability. The UV laser beam was passed through the objective lens on the sapphire material which was mounted on motorized precision X-Y translation stage which controls the material position and scan speed by computer [43].

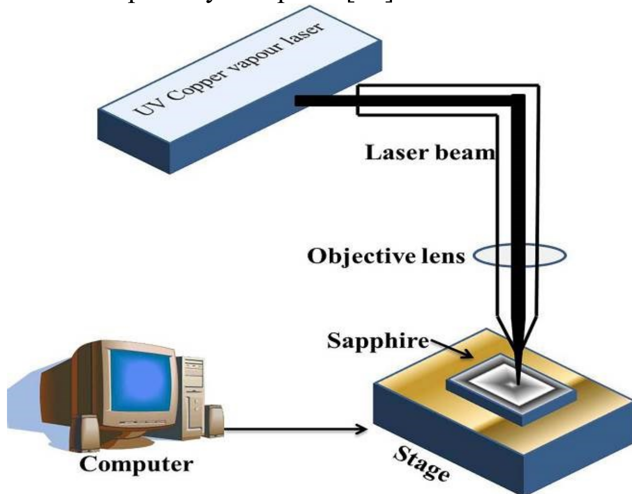

Fig. 12. Schematic diagram of the copper vapour Laser

E. Gu et al. successfully machined and diced the sapphire material by using pulsed UV copper vapor laser at wavelength 255nm. They fabricated well-defined grooves wide up to 30µm and 430µm deep on sapphire which having a high aspect ratio. The UV laser dicing gives high productivity as compared to mechanical dicing process [43].

l. Fluorine Laser

The UV beam from fluorine laser system passed through the shutter and reflected by mirror reached upto homogenizers i.e. A1 and A2 which gives high uniformity to the UV beam then passing to the mask it directed towards the sample which was mounted on worktable moved by NC stages i.e. x, y, z and r which was monitored by computer. The CCD 1 camera monitored the the position of the ablating points while the ablation procedure was monitored by CCD 2 camera. The detailed experimental setup is presented in figure 13. Y. Dai et al. formed 3D microstructure on sapphire material by using 157nm DUV laser micro ablation process. According to them, the 157nm laser etching process gives good quality ablation hence can be used to produce 3D microstructures of many other micro devices [44].

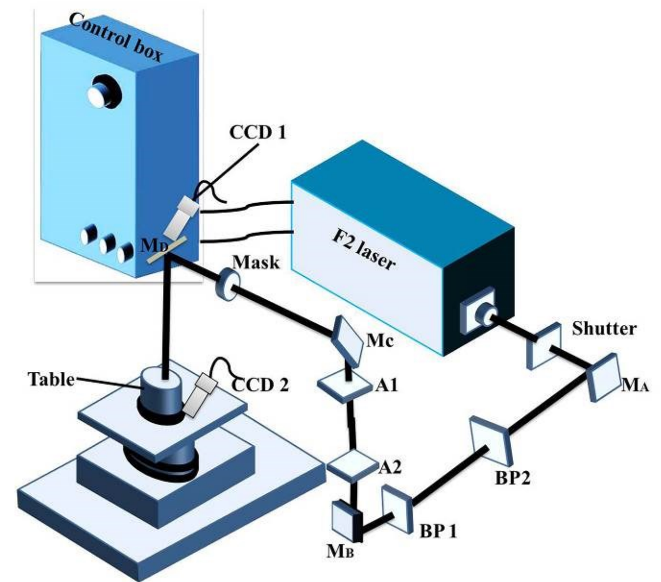

Fig. 13. Schematic diagram of the fluorine laser (Redrawn from [44])

2.2 Grinding Process

The grinding process produces a very fine surface and accurate dimension which is better suitable for machining of hard materials. It has an abrasive wheel and work holding device called as a chuck which is operated by using the vacuum or electromagnetic and a reciprocating table. The abrasive wheel rotated at different speeds and the workpiece may stationary or rotary depending upon types of grinding machine. During the machining process, grinding machine removes material from workpiece by abrasion which produces heat. So, for cooling the abrasive wheel and workpiece coolant is used to eliminate the heat [45-63]. This process includes different grinding methods such as, elliptical ultrasonic assisted grinding, ultrasonic vibration grinding, modified grinding, micro slot grinding, CNC grinding, conventional grinding, Electrolytic In-Process Dressing grinding.

a. Elliptical Ultrasonic Assisted Grinding (EUAG)

In this machining method a grinding unit contiaining elliptical ultrasonic vibrator and holder were attached to the worktable with a dyanamometer. On the top face of the vibrator a thin sheet was attached causes two ways vibration i.e. along the wheel axis and vertical to the work-surface. The rotated grinding wheel interfere with the workpiece resulted into removal of material [45-50]. The schematic diagram of this process is illustrated in figure 14. Z. Liang et al. [45] carried out grinding experiments on sapphire substrate. According to them due to the elliptical

ultrasonic vibrator, the grinding forces, grinding force ratio, surface fractures and cracks get decreased. Whereas, surface roughness improved up to 15%. Hence, it proves that the two dimensional ultrasonic grinding process is the best option to achieve high quality performance from the sapphire substrate.

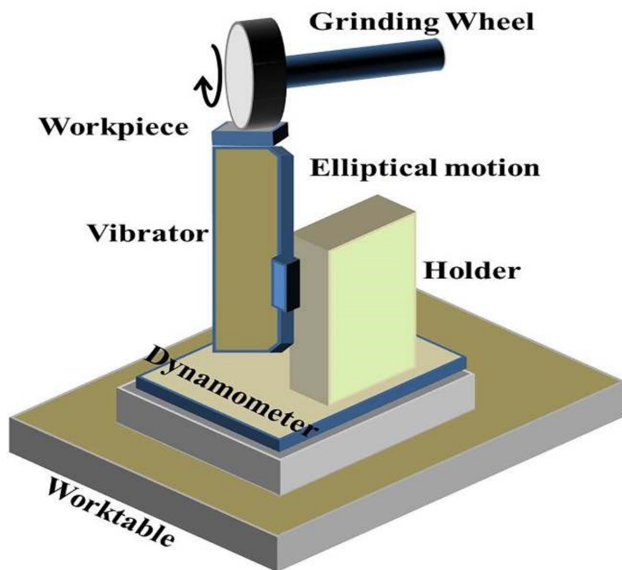

Fig. 14. Schematic diagram of the elliptical ultrasonic assisted grinding (Redrawn from [45])

Z. Liang et al. [46] studied surface formation characteristics of monocrystal sapphire by using elliptical ultrasonic assisted grinding process. They observed surface roughness get decreased up to 25% because of the elliptical vibration in elliptical ultrasonic assisted grinding process as compared to conventional grinding. The improved surface quality was also achieved by elliptical ultrasonic assisted grinding process hence it is the most suitable process for the machining of monocrystal sapphire. Y. Wu et al. [47] used elliptical ultrasonic assisted grinding process for investigating the wear performances of resin bond diamond wheel. The wheel wear process was classified in three regions. In initial and steady region, the grinding forces of EUAG were smaller than conventional grinding (CG). The larger grinding forces were achieved in deteriorated region. The work surface of all three regions was much smoother than CG. The wheel wear observed in CG was due to the attritious wear, macro fracture and abrasive grains pullout, whereas in EUAG it was detected because of macrofacture and abrasive grains cleavage. Z. Liang et al. [48] stated that the EUAG shows improved performance of grinding wheel than the CG, because it shows 20% longer steady region, produce high active cutting edge density which improves surface roughness, also generate micro fracture and abrasive grain cleavage which maintain longer sharpness in EUAG. Z. Liang et al. [49] stated that the EUAG was the most suitable method for the monocrystal sapphire materials because it produces larger critical depth of cut which gives high material removal rate. Q. Wang et al. [50] used structure function method to investigate the surface formation mechanism of monocrystal sapphire in EUAG. They observed that, the EUAG generate fine surface with bigger surface fractal dimension than CG.

b. Ultrasonic Vibration Grinding (UVG)

The figure 15 shows schematic diagram of ultrasonic vibration grinding process. In this process, the coolant was inserted to the inner and outer side of the hollow sintered diamond tool which was rotated in high speed and ultrasonically vibrated and has the transverse reciprocating feed causes grinding operation. The workpiece feed was longitudinally towards the tool.

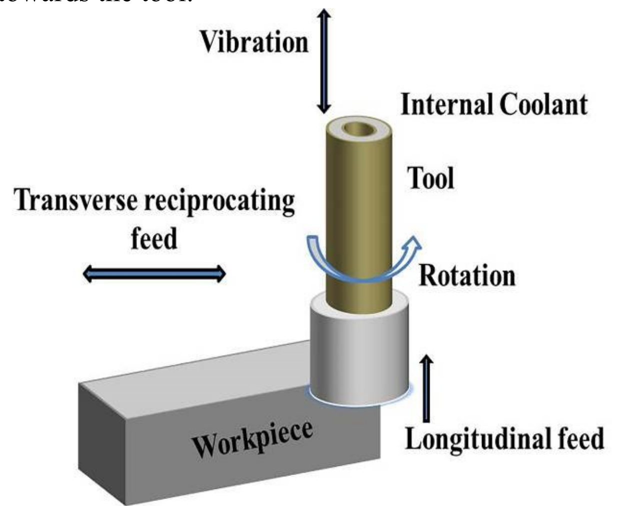

Fig. 15. Schematic diagram of the ultrasonic vibration grinding (Redrawn from [51])

X. Yang et al. used ultrasonic vibration grinding process for hard and brittle materials study. According to them, UVG gives lower machined surface roughness, high material removal rate and small wear extent of tool hence it is more efficient method for the machining of Hard and brittle materials [51]. Z. Liang et al. [52] developed elliptic ultrasonic vibrator on a metal elastic body for sapphire grinding. They observed grinding forces get decreased with improved surface quality. Thus they indicated that this new grinding technique is most efficient for the machining of sapphire substrate.

c. Modified Grinding

The figure 16 shows experimental procedure of modified grinding. The modified gridning process is a modification of conventional grinding process. This process also worked as above grinding processes besides in this process an acoustic emission and high precision dynamometer was mounted on a 5-axis

machine tool. The dynamometer was used for capturing cutting forces and setting the postion of micro cutting edge of grinding wheel [53]. D. Axinte et al. explored single grit micro geometry effects on sapphire grinding. The less accurate replication of grit shape and reduced cross sectional scratch marks was observed due to fracture effect. Whereas, the surface topography shows square, circular and triangular grit [53].

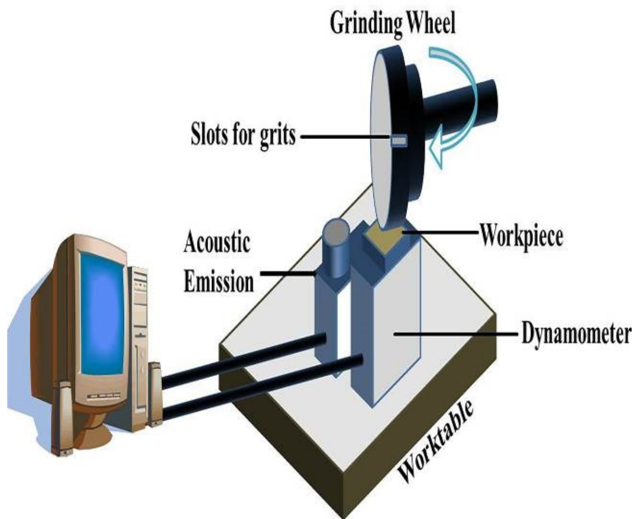

Fig. 16. Schematic diagram of the modified grinding (Redrawn from [53])

The modified CNC milling machine having a spindle with the grinding disk provides x, y and z-axis movement, however workpiece was stationary K. Wasmer et al. experimented with a parametric study and proposed a model for the sapphire grinding. They observed that wheel speed, feed speed and vertical feed were the most influencing parameters for sapphire grinding because the performances of tangential forces, optimization procedure, productivity, grinding quality and material removal rate are dependent on these three parameters. The high material removal rate with good productivity was achieved by the newly proposed model hence it can be used for other brittle materials [54]. A. Voloshin et al. [55] investigated the binding effect in abrasive machining of sapphire by using coolant with different pH. They concluded that the change in pH from neutral to acidic gives a higher grinding rate. Whereas, the alkaline pH provides attrition of the workpiece surface. Hence, changes in coolant pH value from neutral to acidic and alkaline, can increase the efficiency of sapphire machining and also decrease its surface roughness. S. Gao et al. [56] enhanced the sapphire wafer machining efficiency by using conventional loose abrasive process. In this process, they have used fixed abrasive diamond plates with different grain size for sapphire wafer grinding which resulted into removal of surface material. While the diamond plates having abrasive size 40µm produce high MRR

d. Mircro Slot Grinding (MSG)

The micro slot grinding of the sapphire is presented in figure 17. In this process the sapphire workpiece was held on a vacuum chuck in addition to dynamometer was attached to capture the grinding force data. J. Cheng et al. proposed a model for the study of MSG for single crystal sapphire having different orientations. According to their observations the A orientation {1120} shows high grinding force than the C orientation {0001} and R orientation {1102} [57].

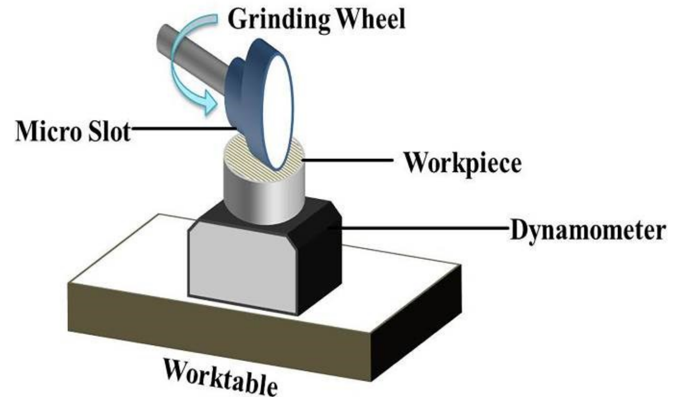

Fig. 17. Schematic diagram of the micro slot grinding

e. CNC Grinding

The precision CNC grinding machine was used to grind the cylindrical blanks of single crystal sapphire of c-axis orientation. The feed, speed and depth of cut of gridning wheel were controlled by computer numerical controlled system. In this grinding operation by the tool orientation they created a plane surface under constant feed control and workpiece speeds. The figure 18 shows schematic diagram of CNC grinding process.

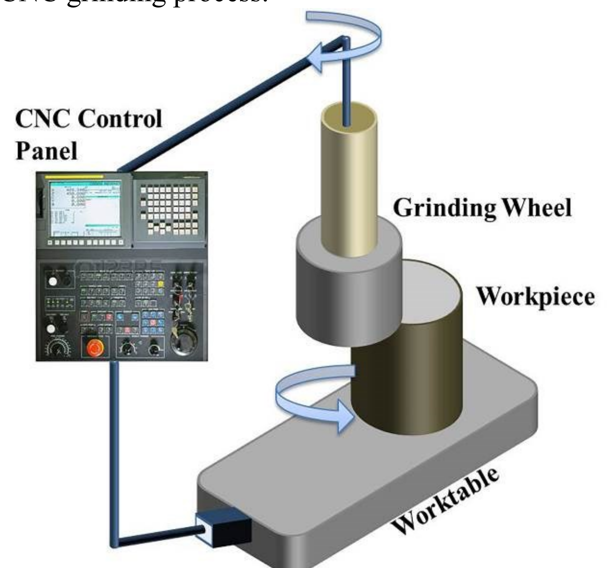

Fig. 18. Schematic diagram of the CNC grinding

P. Funkenbusch et al. produced finely ground surfaces on single crystal sapphire by using bound abrasive cup tools in a grinding process. According to correlation coefficient observations, the workpiece roughness and material removal are influenced by chip thickness [58]. The CNC precision machining operation on sapphire workpieces were cylinders of 52 mm diameter. The flat surfaces were produced on sapphire by plunging the wheel down toward the sapphire workpiece. Y. Zhou et al. used CNC grinding platform for examining vitrified bond diamond wheels in grinding process of single crystal sapphire. The cyclic behavior occurred in machine deflection causes self-sharpening. However, the grinding wheel failure observed because loss of self-sharpening action. The results show that vitrified bond wheel can remove large volumes of sapphire without redressing [59]. D. Funkenbusch et al. [60] correlated grindability with workpiece roughness which will used to comprise workpiece finish in the optimization process and it will help for grindability estimation. It will also important for the development of removal processes. They stated that the grinding process produced natural link between grindability and surface finish.

f. Conventional Grinding

The precision self-rotation grinding machine and resin-bonded grinding wheel used to grind sapphire. The experimental setup for conventional grinding process is shown in figure 19.

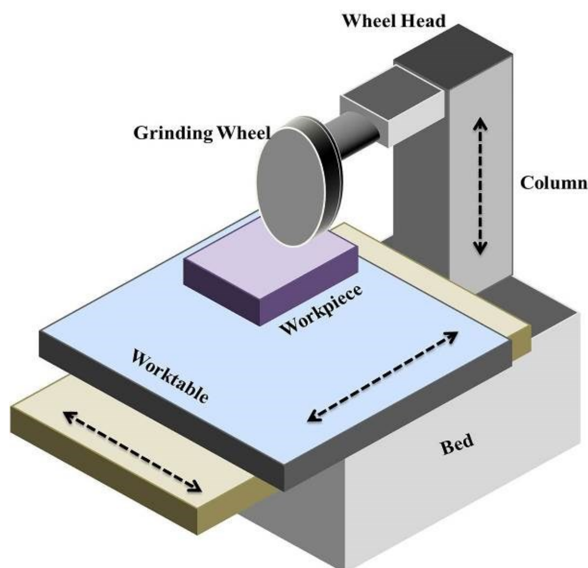

Fig. 19. Schematic diagram of the conventional grinding

H. Zhou et al. studied improved grinding process in which rubber pad added between LED sapphire substrate and worktable forms the cushion grinding by which a high surface flatness was obtained. They observed higher deformation volume in traditional grinding than the cushion grinding. Thus, to grind sapphire substrate efficiently, economicaly and highly automated way the upholstered film is the best option [61]. J. Bashe et al. [62] investigated critical parameters in grinding process during large sapphire window panels. They observed heavier added weight, larger starting grit size and deionized water are the grinding parameters which improved the surface roughness. While the removal rate was improved by the grinding parameters such as the heavier added weight, higher slurry viscosity and faster arm oscillation speed.

g. Electrolytic In-Process Dressing (ELID)

This experimental setup includes CNC with an ELID system, a dynamic balance system, and an acoustic emission system. The copper electrode casing 1/6 of the perimeter for the grinding wheel was used for an electrolytic dressing. The cast iron bond diamond grinding wheel was joined to the positive pole which was mounted on the backside of the grinding wheel. The 0.2mm gap maintained between the wheel and electrode. The acoustic emission signals were sensed by the sensor. The coolant was used as electrolyte. The nozzle provides grinding fluid which was worked as lubricative for ELID. The grinding wheel was operated by pulse power supply and grinding of material surface takes place which is represented in figure 20.

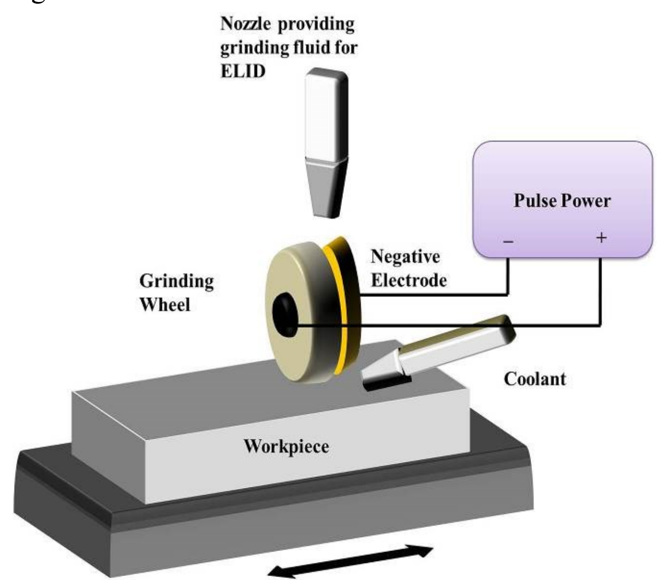

Fig. 20. Schematic diagram of the ELID grinding (Redrawn from [63])

P. Han et al. used acoustic emission for sapphire material grinding. They observed that as the dressing current increases the surface finish also improve. The acoustic emission root mean square (AE RMS) was found to be higher at lower dressing currents. As depth of cut increases the average AE RMS also increases. The high depth of cut in ELID grinding resulted into breakage of oxide layer [63].

2.3 Polishing Process

Polishing is nothing but a finishing process which is used for smoothing a workpiece surface with a polishing wheel and an abrasive. The high-speed polishing machines can be used to obtain the flat, mirror bright finish and defect-free surface. In this process the rubbing or chemical action take place which produces a smooth surface. In polishing process, the abrasives starts with coarse to fine machining method. During the process for the cooling effect lubricants media may be used [64-79]. This process contains various methods of polishing i.e. chemical mechanical polishing, ultrasonic flexural vibration assisted chemical mechanical polishing, Fe-Nx/C-assisted chemical mechanical polishing, chemical mechanical plasma polishing, mechanical chemical polishing, chemical assisted polishing, tribochemical polishing, double sided polishing, hydrodynamic polishing and computer controlled polishing.

a. Chemical Mechanical Polishing (CMP)

The polishing tests were attained by UNIPOL-1502 chemical mechanical polishing machine. The polishing pad was used as Rodel porous polyurethane pad. The sample holder was placed on pad which was mounted on platen. During chemical mechanical polishing slurry feed gives smooth polishing surface to the material which is illustatred in figure 21.

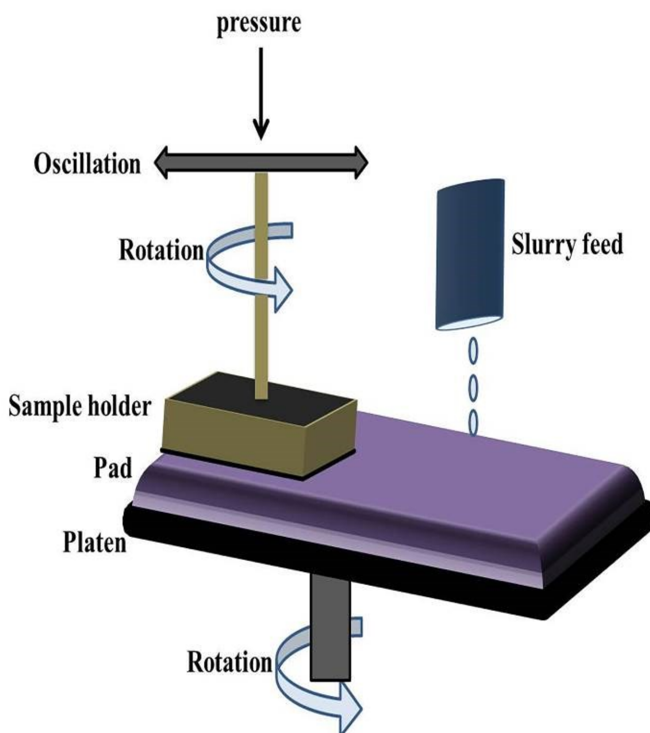

Fig. 21. Schematic diagram of the chemical mechanical polishing (Redrawn from [67])

The influences of Cu-doped and Ce-doped colloidal SiO_2 abrasives on the chemical mechanical polishing performance were evaluated under polishing conditions such as polishing time, down force, plate rotating speed and slurry supplying rate [64, 65]. H. Lei et al. [64] used seed-induced growth method and achieved Cu-doped colloidal SiO_2 composite abrasives. The Cu-doped colloidal SiO_2 considered as polishing abrasive, the resulted abrasive shows low surface roughness (Ra) and high material removal rate (MRR) than the pure colloidal SiO_2 abrasive under the same experimental conditions. H. Lei et al. [65] prepared new Ce-doped colloidal SiO_2 composite abrasives which have good dispersibility and inerratic spherical shape. The low Ra and high MRR were observed in slurries which contain Ce-doped colloidal SiO_2 composite abrasives. The solid chemical raction take place between Ce-doped colloidal SiO_2 composite abrasives and sapphire substrate improves the sapphire chemical mechanical polishing. Z. Zhang et al. [66] reported the mechanical parameters effect on friction force which was measured by the sensor and MRR during the chemical mechanical polishing of sapphire. They observed that the increased rotation speed also increases the polishing rate but at the same time it reduces the friction force as well as coefficient of friction. H. Zhu et al. [67] used aqueous abrasive slurries to study the material removal rate in polishing planes of sapphire. They observed dissimilar polishing performance but show improvement in c-, a- and m- planes of sapphire which was towards the material removal rate. The soft hydration layer formed on a sapphire surface resulted into material removal and provides fine surface quality to the basal plane. The alumina slurry abrasives with pH 12 showed a higher removal rate and better surface finish. C. Park et al. [68] investigated the effect of abrasive size on high CMP pressure of sapphire wafer. They found that the removal rate gets increases with increase in CMP pressure. They also observed that the abrasive size and concentration of the slurry were also affected by material removal rate and the slightly increased surface roughness was noticed. H. Aida et al. [69] studied CMP of sapphire by using colloidal silica slurry with different pH. They achieved atomic level surface flatness and low surface roughness.

b. Ultrasonic Flexural Vibration Assisted Chemical Mechanical Polishing

The figure 22 shows experimental setup for ultrasonic flexural vibration assisted chemical mechanical polishing process. In this process, the piezoelectric transducer transforms the electrical signal into the mechanical vibration signal because of the piezoelectric effect. Then this mechanical vibration signal was amplified and moving to the polishing head by the ultrasonic horn, therefore the rotating polishing head by the

sapphire substrate can vibrate in vertical and horizontal directions. The surface material of sapphire was removed by the combined actions of ultrasonic vibration and traditional chemical mechanical polishing process [70, 71]. W. Xu et al. [70] used ultrasonic flexural vibration assisted chemical mechanical polishing process for material removal and the polished sapphire substrate. According to them, for Sapphire MRR the important factors are silica abrasive and ultrasonic particles. While, the use of chemical additives resulted into reduced roughness in sapphire material. W. Xu et al. [71] obtained larger MRR, better surface roughness and better surface flatness in ultrasonic flexural vibration assisted chemical mechanical polishing (UFV-CMP) process than chemical mechanical polishing (CMP). Thus, the UFV-CMP greatly improves MRR and gives a fine surface quality to the sapphire substrate.

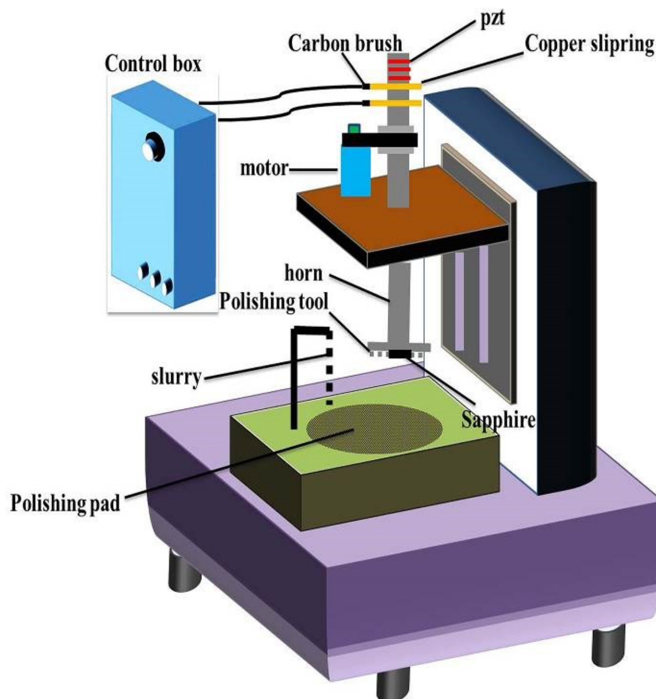

Fig. 22. Schematic diagram of the ultrasonic flexural vibration assisted chemical mechanical polishing (redrawn from [71])

c. Fe-Nx/C Assisted Chemical Mechanical Polishing

The pyrolyzed carbon supported Fe-Nx catalysts were formed by solvent-grinding technique subsequent to the heat treatment at 600°C. So, the catalyst and catalyst free based colloidal silica slurries were prepared for chemical mechanical polishing. The experimental procedure for this process is same as chemical mechanical polishing. L. Xu et al. concluded that the non-noble metal catalyst (Fe-Nx/C) showed remarkable catalytic performance for sapphire in colloidal silica slurry. It effectively improves the material removal rate of sapphire in CMP. It also gives a superior surface finish of about 0.078nm on the basal plane [72].

d. Chemical Mechanical Plasma Polishing Process

The rapid hydration of the sapphire wafer surface obtained by using an atmospheric pressure and low-temperature plasma. The radio frequency power produced plasma to the one powered electrode and humid Helium gas passing between the grounded electrode and a powered electrode. The bubbler containing water utilized to water vapor and introduced into the Helium. Due to water vapour into the plasma the formation of hydroxyl (OH) species was take place, which develop the hydration of sapphire surface. Therefore it reduces the hardness of the top layer and this softened layer was then removed in the chemical mechanical plasma polishing process. The schematic diagram for this process is presented in figure 23. A. Bastawros et al. used chemical mechanical plasma polishing process for the material removal of sapphire [73].

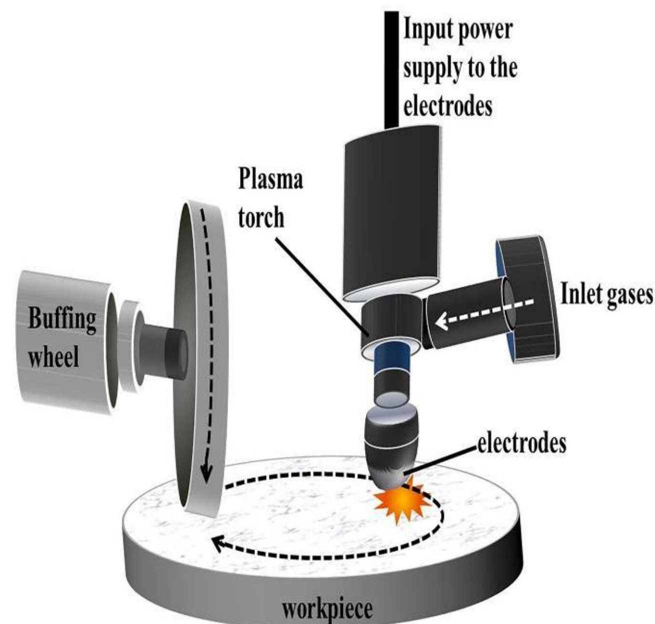

Fig. 23. Schematic diagram of the Chemical Mechanical Plasma Polishing Process (redrawn from [73])

e. Mechanical Chemical Polishing

The figure 24 shows schematic diagram of mechanical chemical polishing. The nano-sized abrasives film of magnesium oxide, silicon dioxide and ferric oxide was used for mechanical chemical polishing. Also the Nanopoli-100 ultra-precision polishing machine utilised for the sapphire polishing experiments and deionized water was used as coolant. Y. Xu et al. studied reactivity between nano-sized abrasives and sapphire wafer in a chemical mechanical polishing process. They observed that the mechanical force causes chemical reaction between silicon dioxide nano-abrasive and sapphire in which

chemical etching was absent. The SiO_2 nano-abrasives show high reactivity as compared to other abrasives in the same conditions [74].

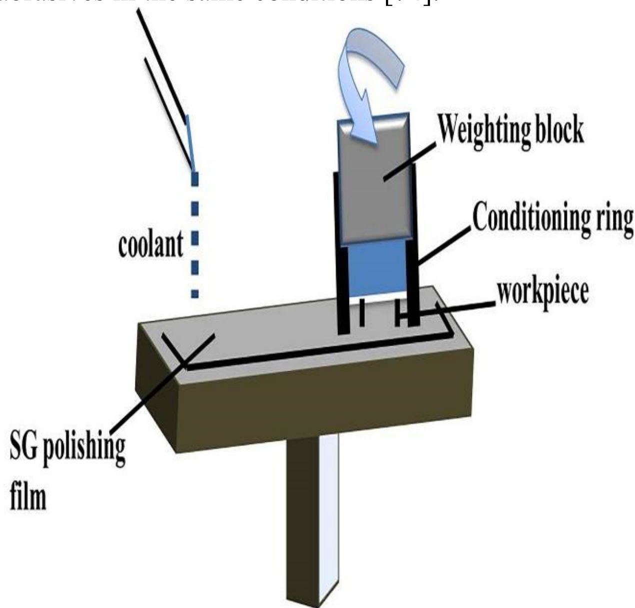

Fig. 24. Schematic diagram of the mechanical chemical polishing (redrawn from [74])

f. Chemical assisted polishing

In this method two polishing machines were used i.e. lapping using a cast iron platen and polishing by an aluminum platen for mounting of polishing pads. The desired pressures was applied on a polishing plate with platen speeds at 60 rpm was kept. The polishing experiments were carried out on *c* plane sapphire with controlled pH and abrasive concentration. The schematic diagram is same as chemical mechanical polishing process. H. Zhu et al. used abrasives of different hardness to study the chemical assisted polishing for finishing sapphire plane. The abrasives having hardness same as or less than sapphire will produce best surface finish and high material removal rate. A thin hydration layer was formed on c-plane sapphire which was removed by softer abrasive which resulted in to high MRR and good surface quality [75].

g. Tribochemical polishing

The experimental setup of tribochemical polishing is shown in figure 25. For this process the grinding and polishing machine was used. The machining zone temperature was increased by electric heater and controlled by the voltage regulator. The workpiece and the tool were continuously dipped into the polishing suspension. This process has done sequentially by coarse, fine, finish grinding and diamond polishing operations on sapphire. Then the tribochemical polishing for 300 min was done [76].

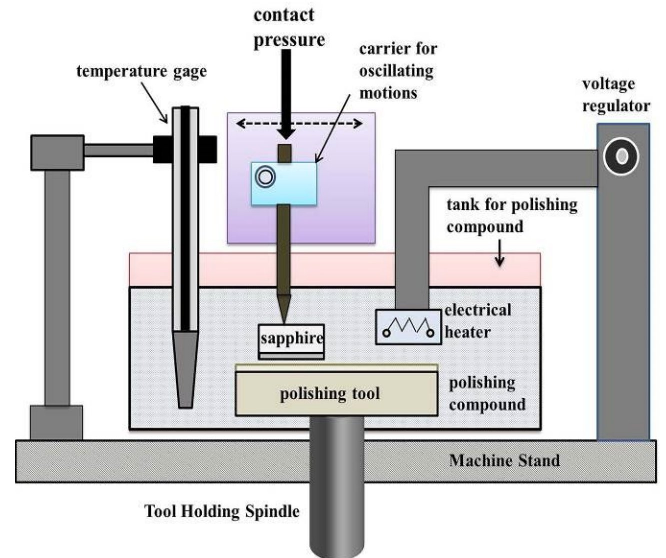

Fig. 25. Schematic diagram of the Tribochemical polishing (redrawn from [76])

V. Rogov et al. observed that in tribochemical polishing process the chemical mechanism occured between α-Al_2O_3 and colloidal silica SiO_2 due to which the material removal gets increased. This chemical mechanism improves the process productivity and decreases labor intensiveness [76].

h. Double Sided Polishing

G. Hu et al. introduced precise double sided polishing machine with special reference to its structure and characteristics. This machine provides stable pressure controls and more powerful and stable driving force compared to lapping process. The schematic diagram of this process is presented in figure 26. The machine has advanced mechanism design, motor movement controlled by computer and accurate pressure control which improves the accuracy and productivity of this machining [77].

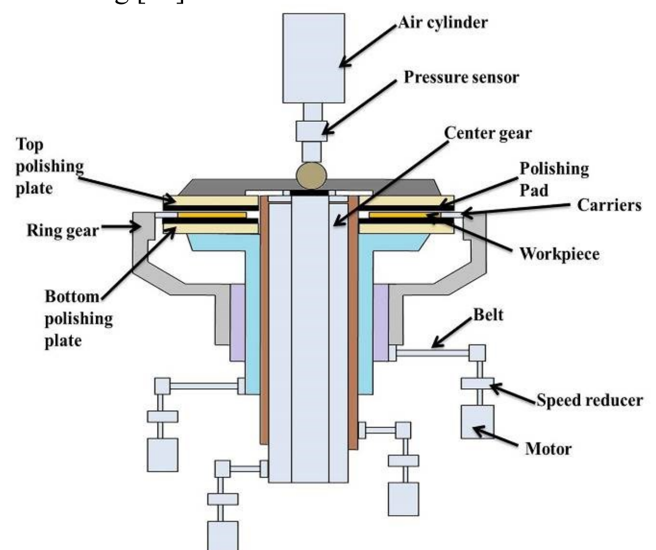

Fig. 26. Schematic diagram of the double sided polishing (redrawn from [77])

i. Hydrodynamic Polishing

The sapphire material was fixed inside an acrylic tank filled with abrasive slurry. This tank was mounted on mini dyanamometer which was fixed on top of the table. The soft silicon cylindrical tool having a 15 mm diameter hemispherical working end was operated by a motor resulted into effective surface polishing. The figure 27 shows experimental setup of this polishing process. P. Kumar et al. The obtained results show that hydrodynamic provides effective flat polishing, it can reduce surface roughness up to 60% and 209nm surface roughness was achieved [78].

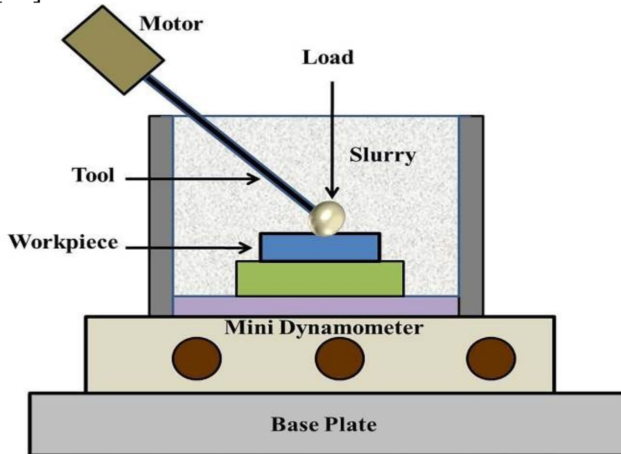

Fig. 27. Schematic diagram of the hydrodynamic polishing

j. Computer Controlled Polishing

The figure 28 shows schematic setup of computer controlled polishing. The combined conventional optical finishing with a computer controlled polishing process. The conventional optical finishing process control the window geometry and removal of gross surface errors, whereas the computer controlled polishing process of wavefront error correction and compensation for the localized index in homogeneities inside the sapphire

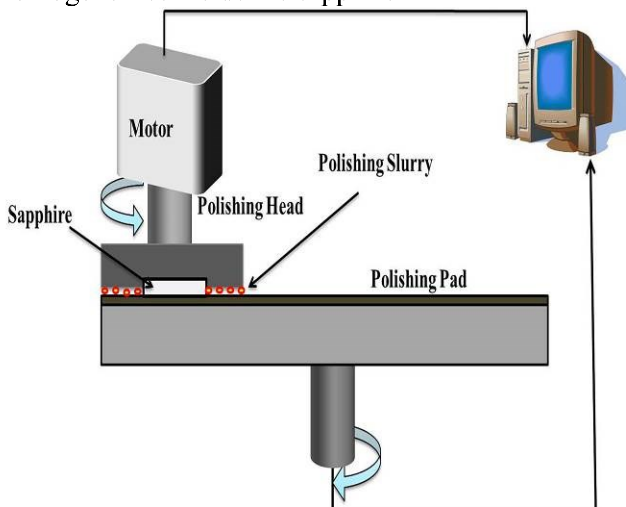

Fig. 28. Schematic diagram of the computer controlled polishing

J. Askinazi et al. produced extreme surface smoothness and low levels of surface microroughness on sapphire by computer controlled polishing process [79].

2.4 Lapping Process

In this process lapping plate and workpiece are rubbed together with the help of abrasive between them via machine or hand movement. The lapping plate is the circular disk located on the top of the machine. The workpiece is positioned below the upper lapping plate. The lapping plate rotates and abrasive slurry feeds by using the slurry pump in between workpiece and lapping plate. The workpiece is placed in work holding plate. The pressure is applied to workpiece during the material removal process. This process is used to make a precise surface roughness and achieved a very accurate flat surface [80-83]. This process is categorised into two type's i.e. single sided and double sided lapping process.

a. Single Sided Lapping

The 3-Body lapping was attained in a single-sided lapping tool with diamond slurry and metal resin platen. Whereas, 2-Body experimented by a fixed diamond abrasive pad by using a low concentration of alumina slurry. The sapphire substrate inserted between rotated resin platen and ceramic holder and diamond slurry was injected between them. The pressure was exerted on the ceramic holder due to which the sapphire substrate get rotated and single sided lapping on sapphire was carried out. The schematic diagram of this process is presented in figure 29. H. Kim et al. compared the 2-body and 3-body lapping process for sapphire substrates. They concluded that fixed diamond abrasive pad is initially designed for 2-body abrasion which contains a lower concentration of diamond abrasives which gives higher material removal rate [80].

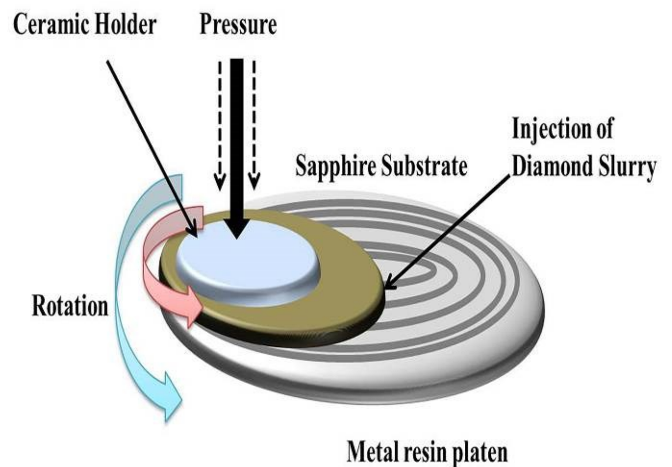

Fig. 29. Schematic diagram of the single-sided lapping (redrawn from [80])

b. Double Sided Lapping

The figure 30 shows schematic diagram of double sided lapping. The double-sided planetary lapping was applied to the c-plane sapphire wafers. These wafers run at low pressures by using SiC slurry, whereas the 2-body process was applied by using diamond TDT and a minimum of three times the pressure used and double sided lapping was takes place [82].

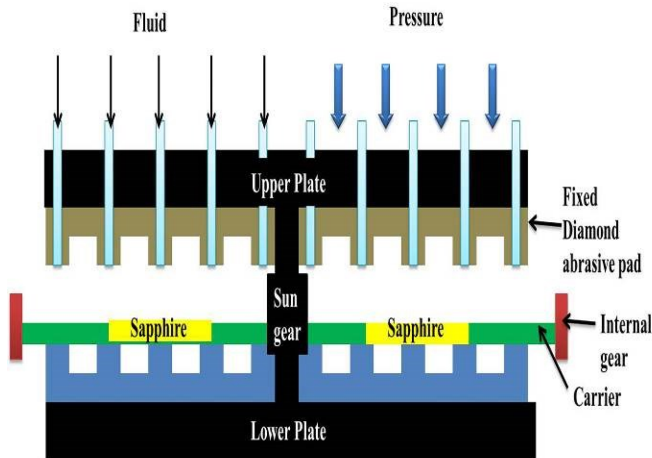

Fig. 30. Schematic diagram of the double sided lapping (redrawn from [82])

J. Gagliardi et al. found better results of material removal rate, subsurface damage and surface finish for a 2-body ductile removal of sapphire compared to 3-body testing in the lapping process. According to them, when ductile mode of material removal can be used as a brittle mode it can produce low subsurface damage on the sapphire. The 2 body testing is with 80 µm Diamond TDT (Trizact Diamond Tile) at 3×the psi resulted into fine surface finish across the entire wafer, shallower scratches and lower surface stresses [81]. A double-sided lapping machine with a fixed diamond abrasive pad with low concentration of alumina slurry and Triethanolamine was used as a dispersant. H. Kim et al. concluded that for obtaining higher sapphire material removal rate, the synergetic action of diamond particles and alumina abrasives are important factor. The material removal of lapping process is linearly dependendent on pressure and speed. They achieved 1 µm/min material removal rate with good surface quality [82]. The sapphire samples were dual lapped with boron carbide abrasive having the rotational speed of 7.5 rpm and the lapping pressure of 0.1Mpa. K. Zhang et al. explored the material removal mode and ratio involved in dual lapping process by studying the machining characteristics and moving style of abrasive used for sapphire wafer lapping. They observed that the grains dislodgement caused by micro-cracks occurred on grain boundaries was the main reason of material removal for this material. According to them, this process will be used to improve the ceramic lapping process, enhances surface quality, microstructure designing of future sapphire, increases productivity and produces economic sapphire material for industrial applications [83].

2.5 New Developed machining process

It is modified existing setup for obtaining better machining performance. In this experimental setup, the innovative application of technologies, processes and methods are applied by which the performance of machine efficiency and product quality can be improved [84-88]. The atomic force microscopy (AFM) probe as a cutting tool, high speed ductile Machining, rotary ultrasonic drilling, manufactured dicing blade for dicing machine are the newly developed process for machining of sapphire.

a. Atomic Force Microscopy Cutting Tool

The atomic force microscopy made by Veeco Digital Instruments Inc. used for nanoscale cutting. The diamond coated probe was utilized to prevent from braking, deformed and worn during cutting action by a probe. The tip of the probe performed like a semispherical cutting tool. The normal spring constant of the probe of Atomic Force Microscopy scanned by the computer and the actual resonance frequency of the probe was analyzed. The schematic diagram of this process is shown in figure 31. [84, 85].

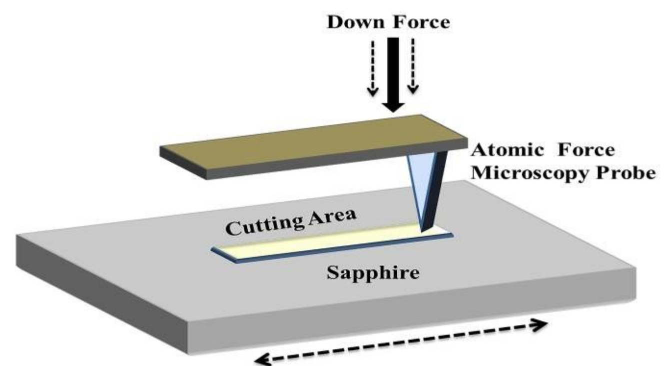

Fig. 31. Schematic diagram of the atomic force microscopy cutting tool (redrawn from [84])

Z. Lin et al. [84] the results obtained from this theory are compared with actual nano cutting results which are obtained by the AFM probe. They observed that the results obtained from this theory were very close to the results obtained from practicle experiments having same down force and cutting passes number. Thus, according to them, a desired cutting depth can be achieved by using specific down force energy theory. J. Huang et al. [85] tested nano-line machining and nano-rectangular pattern machining at different normal force for single crystal sapphire by using atomic force microscopy. A nano-line

machining test shows increased groove depth as normal force increases in ductile regime cutting model. While in nano rectangular pattern machining test as normal force increases the groove depth also increases with small chips accumulation in the brittle regime cutting model.

b. High Speed Ductile Machining

In this process the HT amplifier used to amplify electric signals which generates thrust forces to the piezoelectric pusher due to which the sapphire sample get thrust into the track of rotating diamond tool. The comparator was used to measure the cutting speed measured. The figure 32 presents experimental set up of high speed ductile machining. M. Schinker developed an experimental setup for ductile machining of sapphire material by using monocrystalline diamond cutting tools. He observed at 50m/s cutting speed give extremely high temperature during the cutting process. According to them the micro ripple pattern, residual stresses observed on subsurface and microcracks are the factors which limit the surface quality [86].

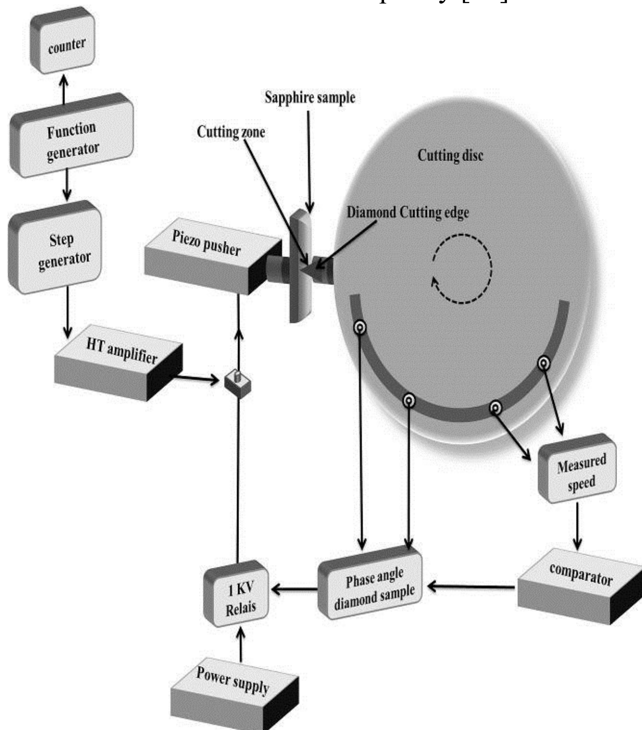

Fig. 32. Schematic diagram of the high speed ductile machining (redrawn from [86])

c. Rotary Ultrasonic Drilling

In this drilling the ultrasonic spindle system was used which includes ultrasonic spindle and power supply. The electrical input was converted into ultrasonic mechanical vibrations by using piezoelectric transducer. The electroplated hollow, diamond tools having wall thicknesses of 1 mm with a diamond grit concentration of 100 were used. The processing fluid used for cooling purposes. The fixture was mounted on dyanamometer which was attached to the table for holding the sample. The electrical signals of dyanamometer get amplified by using amplilier and after that it fed to the data recorder. The recorded data was displayed on computer. The sampling frequency 100 Hz was set for cutting force. The experimental set up of rotary ultrasonic drilling is given in figure 33. J. Wang et al. developed an analytical model for predicting the size of edge chips during rotary ultrasonic drilling (RUD) with special reference to the effect of cutting force and subsurface cracks. They observed increased edge chipping size also increase spindle speed and feed rate. This drilling process produces weak cutting forces, small subsurface crack as well as small edge chips hence it is the superior method for hole manufacturing in brittle materials [87].

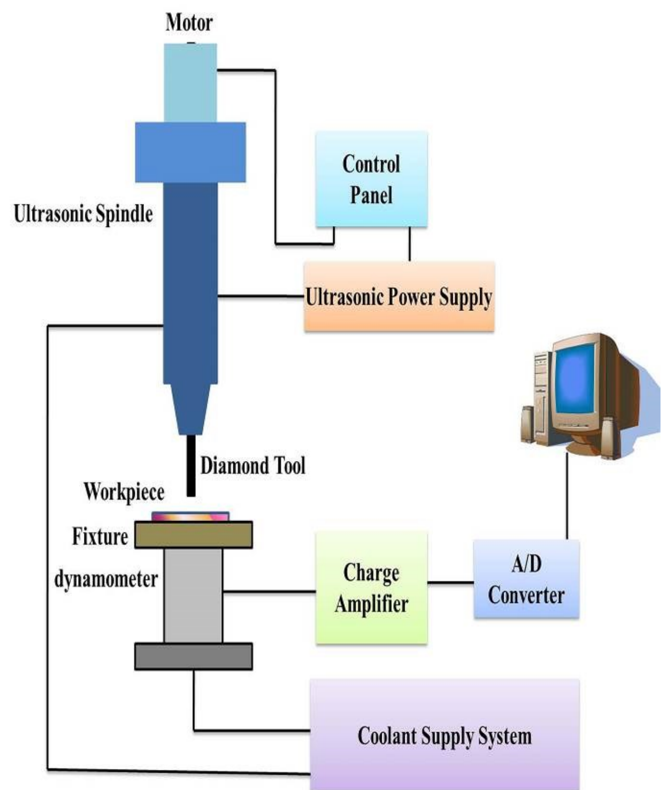

Fig. 33. Schematic diagram of the rotary ultrasonic drilling (redrawn from [87])

d. Developed Dicing Blades

The manufactured dicing blade which was thin and made up of a vitric material having pores. The cutting velocity was 20,000 min^{-1} and feeding rate was 1 mm s^{-1} resulted into 200 mm cutting depth at the initial line. The schematic diagram of this process is presented in figure 34. K. Matsumaru et al. found that the cutting performance of commercial dicing blades depends on the sapphire orientation. The wear of the manufactured dicing blade was larger and it has a high cutting ability [88].

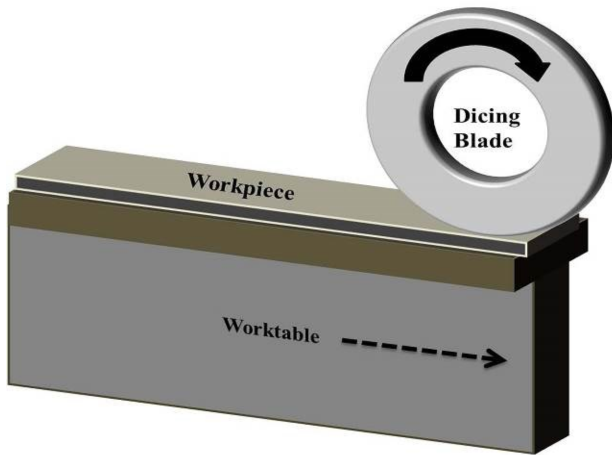

Fig. 34. Schematic diagram of the dicing blade

2.6 Compound Machining Process
The compound machining process is an integrating different machining process which used to achieve the higher machining performance such as surface roughness, material removal rate, and tool wear. The combined different machining process provides more advantageous features for obtaining better results than that of the individual machining process [89-95]. This process includes sequential machining, micro laser assisted machining, ultrasonic vibration assisted machining, combined machining of electrolytic in-process dressing grinding and chemical mechanical polishing.

a. Sequential Machining
In this machining different processes were used sequentially to obtain the better results. This machining contains two step sequencing, three step sequencing and five step sequencing processes. The flow chart for this machining process is presented in figure 35.

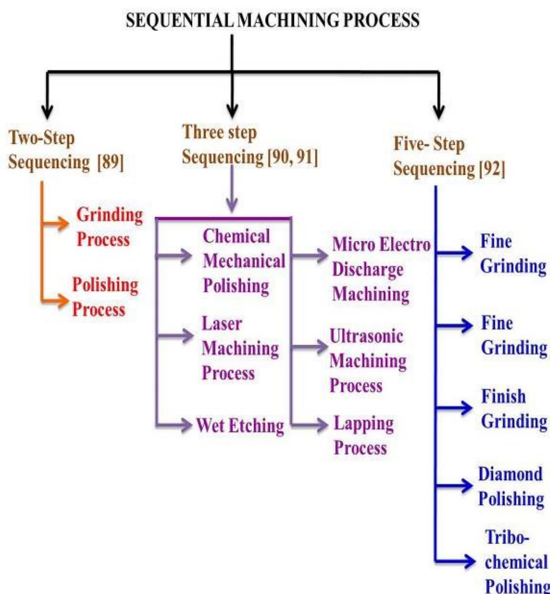

Fig. 35. flow chart of the sequential machining process

The planarized of sapphire material by using grinding and polishing two-step machining processes for which micrometer B_4C and nanometer silica taken as abrasives. Then the ground wafers was polished with the help of colloidal silica as abrasives. The polyurethane polishing pad was used. The pH of colloidal silica slurry was regulated by adding NaOH, H_2SO_4 and H_3PO_4. The feed rate of slurry rises as the rotation speeds up. X. Hu et al. In grinding process the large size and irregular shape of B_4C abrasive create textures and deep trenches. The smaller size and regular shape of B_4C abrasive enhance the planarization efficiency. In polishing process silica nano-abrasive particles are used to polish the ground sapphire wafer and resulted into precise flatness of less than 1nm [89]. The sapphire material polished firstly by using chemical mechanical polishing earlier the edge was chamfered by a picosecond laser and then different processes of wet etching was applied i.e. wet etching by dilute hydrofluoric acid and dry plasma etching. The Residual stresses were analyzed by laser curvature method at different stages of machining. S. Wu et al. concluded that dry and wet both etching process has ability to relief the residual stress without damaging transparency of sapphire glass [90]. Combined three batch mode machining process i.e. micro ultrasonic machining, lapping and micro electro discharge machining process to manufacture the concave and mushroom-shaped spherical structures. The micro-EDM process used to produce the tool for the micro ultrasonic machining process. Then micro ultrasonic machining and lapping process successfully formed desired concave and mushroom-shaped spherical structures. T. Li et al. They achieved 24 $\mu m\ sec^{-1}$ machining rate for the fabrication of concave and mushroom-shaped spherical structures [91]. The obtained coarse and fine grinding process on sapphire by using elastic and soft polishing tools made up of polyurethane or chamois. The process exhibits a diamond abrasive cutting mechanism to a tribochemical interaction between a polishing compound and sapphire. V. Rogov et al. The five sequential machining operations used for this study were coarse grinding, fine grinding, finish grinding, diamond polishing and tribochemical polishing. They observed the surface roughness, affected layer depth, Kikuchi lines and surface texture of sapphire machined surface [92].

b. Micro Laser Assisted Machining
The experimental micro laser assisted machining setup was used to perform scratching test on sapphire. They used IR diode laser with 1070 nm wavelength Gaussian profile and the focused a beam diameter of ~10-20 μm. The IR laser beam was passed through the diamond tool which affects the sapphire material.

The diamond cutting tool having 1 mm nose radius with -45° rake and 5° clearance angle which provides speed as low as 1 μm/sec at nanometric cutting depths. The schematic diagram for this process is presented in figure 36.

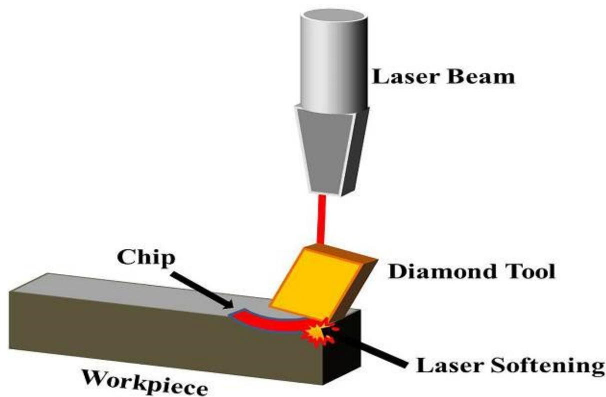

Fig. 36. Schematic diagram of the laser assisted machining (Redrawn from [93])

H. Mohammadi et al. studied the anisotropy effect during ductile mode cutting of the monocrystal C-plane sapphire by using the micro-laser assisted machining process. To perform the scratch tests they have taken monocrystal sapphire having four different perpendicular directions. They observed during cutting operation the fracture has occurred due to which the deepest cuts in [1100] direction were achieved without the tool wears [93].

c. Ultrasonic Vibration Assisted Machining

The rotary motion of the diamond indenter was used in the ultrasonic vibration assisted machining to perform scratch test on the sapphire workpiece. It consists of hybrid mechanism i.e. horizontal feed and ultrasonic vibration. The ultrasonic frequency applied as 19.55–19.75 kHz. Then this workpiece was ground and polished with colloidal silicon dioxide polishing slurry having the particle size of 40–70nm. The figure 37 presents schematic diagram of this process.

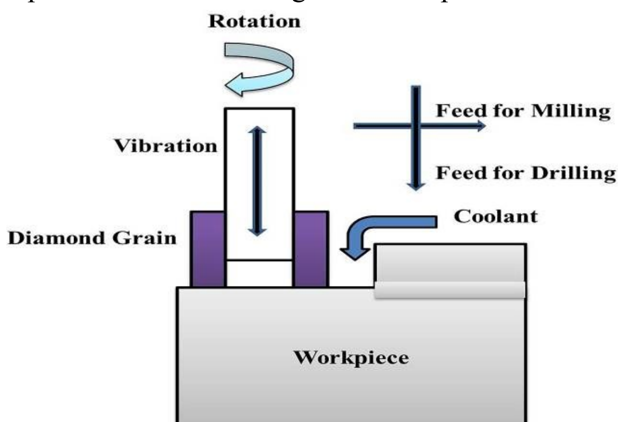

Fig. 37. Schematic diagram of the ultrasonic vibration assisted (Redrawn from [94])

C. Zhang et al. compared the traditional scratching process with ultrasonic vibration-assisted scratch process. They observed that this process reduce the scratch load, prevents microcrack propagation as well as increases plastic removal proportion [94].

d. Electrolytic In-Process Dressing (ELID) Grinding And Chemical Mechanical Polishing (CMP)

The developed a sequential process of electrolytic in-process dressing (ELID) grinding and chemical mechanical polishing (CMP) for the sapphire material used in LEDs. The flow chart of this process is given in figure 38. The ELID grinding having 3 steps i.e. (i) the precision truing of a micro-grain grinding wheel (ii) the pre-dressing process of the wheel using electrolysis and (iii) the grinding process by electrolytic in-process dressing. The feed rate of 1 mm/min was controlled by using a numerical control program. Then CMP process was conducted by applying a POLI 400 polisher. In chemical mechanical polishing, they used mixed abrasive slurry and a polymer impregnated felts type polishing pad and potassium hydroxide based colloidal silica slurry.

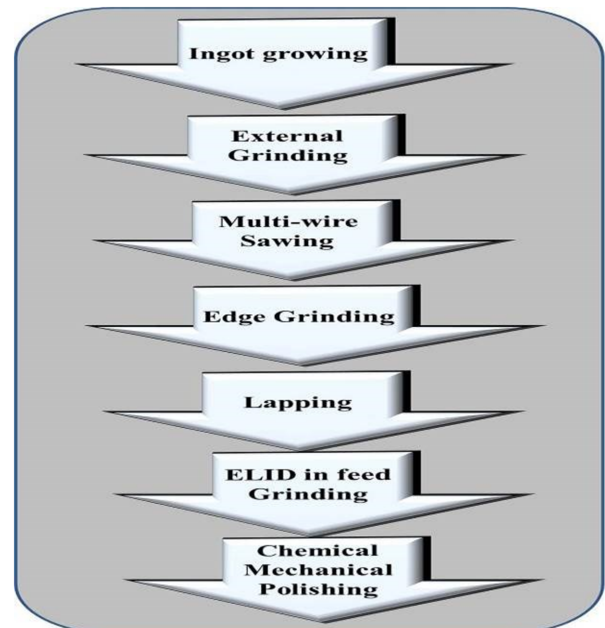

Fig. 38. Flow chart of the electrolytic in-process dressing grinding and chemical mechanical polishing (Redrawn from [94])

H. Lee et al. The process shows reduction in processing time and achieves high surface quality by adopting ELID grinding instead of general mechanical polishing. The high mechanical abrasion and superior scratch removing ability of the mixed abrasive slurry CMP process resulted into a fine surface for hard–brittle materials [95].

2.7 Electro Discharge Machining (EDM) Process

The electro discharge machining is a non-conventional machining process which generates the electrical spark having thermal energy resulted into removal of material. The electrical discharge machining is also called as spark eroding machining process which used to obtain the desired shape and it is also known as electro-thermal process. In this process, a potential difference occur between the tool (cathode) and workpiece (anode), whereas workpiece material to be a conductive material. Both tool and workpiece dipped into dielectric medium called as EDM oil. The gap between tool and workpiece is maintained. The great number of electrons transfers from the tool to workpiece called as avalanche motion of electrons. This transformation of electrons and ions generates the spark. Due to continuous sparking the very high temperature created which causes material removal. The figure 39 shows detailed process of EDM. This process consists of continuation and discontinuation potential difference between tool and workpiece cycle happened. The workpiece gets opposite shape that of the cutting tool.

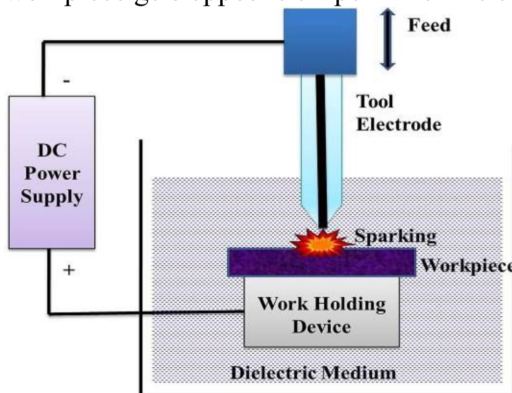

Fig. 39. Schematic diagram of the electro discharge machining

A. Muttamara et al. developed the new machining method for sapphire material by using EDM which was called as assisting electrode method. The copper bar was utilized as the tool electrode and carbon baked layer used as an assisting electrode. The input process parameters was pulse interval time, open load voltage, discharge current, discharge duration, tool rotation speed and jump motion. They discussed crystal orientation effects on sapphire machining properties. They observed high removal rate on (0001) basal C plane with high thermal property. As crystallography varies the machining properties also show variation [96, 97].

3. BRIEF OVERVIEW OF SAPPHIRE MACHINING PROCESSES

The brief overview of machining processes used for the sapphire material was presented in the tabulated format in Table 1. This table contains a brief review of sapphire material research work carried out during last 30 years. It shortly describes the input parameters and achieved results from the seven machining processes used for sapphire material.

The figure 40 shows the yearly progress report of research work carried out on sapphire material by using seven different machining processes.

This bar graph represents the status of sapphire publications from year the 1989 up to 2017. It was observed that the preliminary work was carried out by laser, polishing and grinding processes and these are the mostly used machining processes for sapphire material throughout the journey of sapphire machining.

Table 1. Review of sapphire machining processes

No.	Machining Process	Input process parameters	Results obtained
1	Laser Machining Process	Workpiece material, types of laser, Wavelength [18-44], Repetition rate [18-26, 28, 29, 31, 33-40, 42-44], Pulse duration [18, 20, 21, 23, 24, 30, 35, 36, 38, 44], Output beam diameter [18, 19, 21, 23, 27-29, 31, 33, 40], pulse energy [18-21, 23, 26, 27, 30, 31-34, 36-40, 43, 44], Power [18, 20-23, 25, 26, 28, 29, 31, 33, 34, 36-39, 43, 44], Focal length [18, 20-24,27-29, 31, 35, 37], Pulse width [19, 27-30, 33, 37, 39, 43], Fluence [19-21, 24-27, 30, 32, 33, 38-44], Pulse length [22, 23, 32], Scan Speed, [22-26, 28-30, 33, 37-40, 43, 44], Incident angle, Scanning patterns [37], Absorbing liquid chemical, concentration [41, 42], Chemical [44]	Ablation rate [18, 19, 22, 23, 25, 26, 32, 35, 40, 41, 44], High quality Ablation [18-20, 32, 35], Manufactured laser-induced periodic surface structures [19, 21], Surface morphology [21, 24-26], Smooth and Clean features [22, 23, 30], Scribed and cut sapphire wafer [28, 29, 33], Surface Roughness [30, 37, 42, 44], Process efficiency [33, 34], Aspect ratio [36, 43], Ablation efficiency, Fabrication of linepatterned Superwetting surface on sapphire [24], Precision micromachining [26], Formation of hole key [27], Developed mathematical model [31],

			No micro-cracks, minimal debris or recast layer [34], manufactured deep micro-and nanostructures [36], Morphological and structural modifications [38], Micron-resolution patterning, Ablation depth [39], Surface grating patterns [40], Fabricated three dimensional micro-structure [41], Etch rate [42], Fabricated well-defined grooves [43], Three dimensional micromachining [44]
2	Grinding Process	Workpiece material, Tool/Grinding wheel material [45-63], Coolant [45-52, 55, 56], Voltage amplitude [45-50, 52], Voltage frequency [45-50, 52], Voltage phase difference [45-49, 52], Vibration amplitude [45-49, 52], Tool/Grinding wheel speed [45-52, 54, 56-59, 62, 63], Worktable feed rate [45-50, 52], Grinding depth of cut [45-50, 52, 53, 63], Work Speed [56, 58-60], Infeed rate [58-60], Bending vibration amplitude, Longitudinal vibration amplitude [50], Diamond abrasive grit designation, Longitudinal feed of workpiece, Transverse speed of tool, Vibration frequency of tool, Vibration amplitude of tool [51], Acoustic emission, Number of cutting edges, Grit size [53], Feed speed, Vertical feed, Ultrasonic assistance, Crystallographic direction [54], Grit size, Spindle speed, Loads, Coolant ph [55], Crystal orientation types , Micro-slot grinding depth, Spindle rotation speed, Feeding speed [57], Abrasive size, Grinding plate diameter, Grinding pressure, Coolant flow rate [56], Initial finish, Infeed time [58], Load [61], Weight added, water type, Starting grit size, Arm oscillation speed, Slurry pH, Slurry viscosity type [62], Feed rate, Initial ELID current [63]	Surface roughness [45, 46, 51, 55, 56, 58-60, 62], Machining efficiency [45, 52, 55], Surface quality [46, 52, 56, 60, 63], Material removal rate [54, 56, 58, 60, 62], Tool Wear [51, 58, 59], Investigated wear behaviors of Grind wheel, wear mechanism [47, 48], Critical depth of cut, Material removal ratio [49], Surface formation mechanism [50], Material removal mechanism, specific cutting force [53], Productivity [54], Grinding Force [57], Flatness by FEA [61], Surface stress, Sub-surface damage, Acoustic emission root mean square [63]
3	Polishing Process	Workpiece Material, Abrasive material, Abrasive size [64-76, 78], Down force or Pressure [64-75, 78], Polishing Pad Material, Pad rotation speed, slurry feed/flow rate [64-73, 75], Chemicals [64-76], Abrasive Concentration [64-70, 72-76], polishing time [64-66, 68], Spindle/tool speed [74, 76, 78], Processing time, Coolant [74], Platen rotation speed, Diameter of platen [69,73,75], Atmospheric pressure, plasma, gas, Electrode, electrode length, and Gap [73], Number of double Oscillating motions of the carrier, Polishing compound temperatures [76], Feed rate, Depth of cut, Workpiece rotation speed [78]	Material Removal Rate [64-73, 75, 76], Surface roughness [64, 65, 67-73, 75], Surface Quality/finish [70, 71, 75, 78], Flatness [71], Formation of aluminum silicate with the Composition mullite [74], Process efficiency [76], Friction Force, Coefficient of Friction [66], Fabricated of sapphire windows [79]
4	Lapping Process	Workpiece material, Lapping tool material, Tool size, Abrasive material, Abrasive size, Speed, Pressure [80-83], Lapping Time [80, 82, 83], Abrasive concentration, platen material, platen	Material removal rate, Surface quality/finish [80-83], Surface Roughness [80, 82, 83], Subsurface damage [81, 83]

		speed [80, 82], Standard Speed Fam [81], Triethanolamine [83]	
5	New Developed Machining Process	Workpiece material, Tool material [84-88], Resonance frequency, Normal spring constant, Down force, Number of cutting passes [84, 85], Feed rate [86-88], Speed, Depth of cut [86], Spindle speed, Ultrasonic amplitude [87], Turning velocity, Cutting depth, Cutting directions [88]	Volume of material removed, Cutting Depth [84], Groove depth, Concave depth, Nano-line machining and Nano-rectangular Pattern machining [85], Surface finish/ quality [86], Edge chipping size, Cutting Force [87], Blades wear, Cutting performance [88]
6	Compound Machining Process	Workpiece Material, Tool material/Wheel material/Pad material [89-95], Polishing Pad material, size [89, 95], Speed [89, 92, 95], Abrasive Material, Slurry material and slurry size, Chemical, Slurry pH, Pressure, Slurry Feed rate [89, 94, 95], Ultrasound generator frequency, Ultrasound vibration amplitude, Abrasive material, Machining load, Average machining rate, Cutting depth [91], Normal force, Grain size [92]. Cutting length, Speed of cutting, Laser output power, Cutting directions, Constant thrust forces, Increasing thrust force [93], Ultrasonic frequency, ultrasonic amplitude, scratch velocity, horizontal feed [94], Workpiece rotation, Power, Open voltage, Peak current, Pulse timing, Mixed abrasive, Platen rotation, Head rotation [95]	Material removal rate [89, 94, 95], Surface roughnes [89, 92, 95], Coefficient of friction [89, 94], Reducing Residual Stresses [90], Tool wear ratio, Machining rate, Fabricated concave and mushroom shaped spherical structures [91], Affected layer depth [92], Depth of cut [93], Scratch load [94], Surface finish [95]
7.	Electric Discharge Machining Process	Workpiece Material, Tool electrode material, Assisting electrode material, Discharge current, discharge duration, pulse interval time, open load voltage,tool rotation speed [96]	Material removal rate, surface roughness [96]

Whereas in recent years the compound, new developed and lapping processes are mostly used for sapphire material as it exhibits advanced technology. The EDM is mainly used for the machining of conductive and composite materials, but the sapphire is a nonconductive material hence it observed to be very less used for sapphire material.

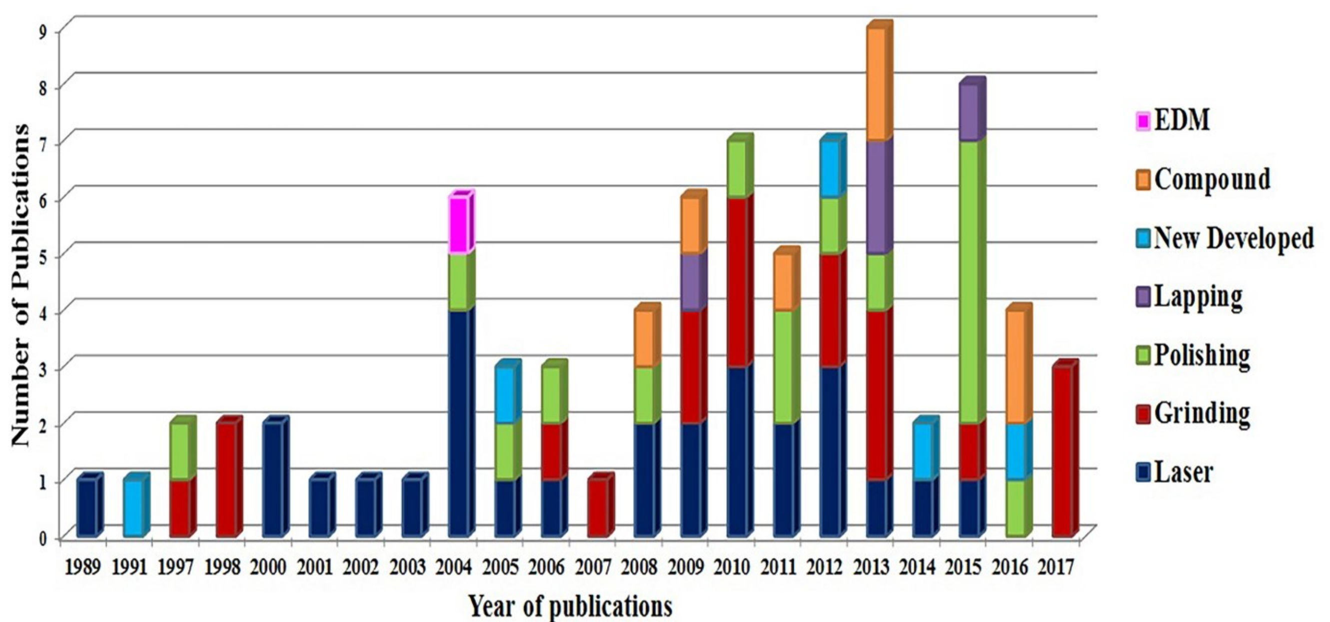

Fig. 40. Progress in sapphire machining processes

4. CONCLUSIONS

The paper has provided a literature review of various processes used for machining of sapphire material. The last 30 years research work of sapphire material has been scrutinized with special reference to the input parameters and achieved results for each machining process. From this review, it is observed that the laser machining process, grinding process and polishing process are mostly used processes for sapphire material. While the EDM is less applicable process or it may be an area for future research. Thus, from this study some important conclusive remarks are made are as follows.

- The overall performance of Laser machining process is better than the other processes as it gives maximum depth. The Ti:Sapphire laser followed by Nd:YAG laser and solid state laser gives the uniform, deepest and high ablation rate which produces smooth and clean surface without damage.
- The elliptical ultrasonic grinding is the most suitable method for grinding of monocrystal sapphire and it is the best option to obtain high quality machining performances. Whereas, ultrasonic vibration grinding is the more efficient method for machining of hard and brittle materials as it gives low surface roughness with high MRR.
- In polishing process, the overall performance of UFV-CMP is better than other polishing methods as it greatly improves MRR and gives fine surface quality.
- The double-sided lapping can provide better result for MRR, surface damage and surface finish.
- The rotary ultrasonic drilling is a new developed machining process and it is the superior method for hole manufacturing in brittle materials. While by using atomic force microscopy one can cut the sapphire material at nanoscale.
- In compound machining process the sequential use of two-step machining gives precise flatness. Whearas, the combined use of three batch mode process can successfully fabricate the spherical structure of sapphire. The micro laser assisted machining gives deepest cuts and enhances the tool life.

5. FUTURE SCOPE

1. The software based finite element modeling or analytical based modeling has been not yet used to predict the output results so it can be applicable for these processes.
2. The various non-conventional machining processes except laser and ultrasonic machining not yet used to machine sapphire material, so this may be a new task for further research work.
3. The hybrid machining processes are the new trends in advanced machining, however very less literature available in this field. Hence, more study is require for obtaining better results in this area.

6. REFERENCES

1.Santos, F., San-Juan, M., Martin, O., Lopez, R., Sanchez, A., Negoescu, F., (2011). *Study of the variation of mechanical properties and cutting forces as an effect of machinability improvement*, International Journal of Modern Manufacturing Technologies, 3(2), 97-104.

2. Slatineanu, L., Dodun, O., Coteata, M., Goncalves-Coelho, A.M., Besliu, I., Pop N., (2009). *Machining methods based on the impact effects*, International Journal of Modern Manufacturing Technologies, 1(1), 83-88.

3. Cohal V., (2009). *Advanced researches concerning lapping process*, International Journal of Modern Manufacturing Technologies, 1(1), 31-34.

4. Mikhailov, A., Sydorova, E., Selivra S., (2012). *Functional-oriented approach for analysis of physical-mechanical processes in the cutting zone*, International Journal of Modern Manufacturing Technologies, 4(1), 85-90.

5. Scheel, H.J., (2000). *Historical aspects of crystal growth technology*, Journal of Crystal Growth, 211, 1-12.

6. Tatartchenko, V., (2005). *Sapphire Crystal Growth and Applications, Bulk Crystal Growth of Electronic, Optical & Optoelectronic Materials,* John Wiley & Sons, Ltd., 300-338.

7. Akselrod, M.S., Bruni F.J., (2012). *Modern trends in crystal growth and new applications of sapphire*, Journal of Crystal Growth, 360, 134–145.

8. Harris D.C., (2003). A peek into the history of sapphire crystal growth, Window and Dome Technologies VIII, Proceedings of SPIE, 5078, 1-11.

9. Harris, D.C., (2004). *A Century of Sapphire Crystal Growth,* Proceedings of the 10th DoD Electromagnetic Windows Symposium Norfolk, Virginia, 1-56.

10. Klejch, M., Nemec, M., Kubat, J., Polak, J., (2013). *Preparation, properties and application of sapphire single-crystal fibers grown by the EFG method*, EPJ Web of Conferences, 48 (00007), 1-5.

11. Dobrovinskaya, E.R., Lytvynov, L.A., Pishchik V., (2009). *Sapphire: Material, Manufacturing, Applications,* Springer US, 1-471.

12. Li, Z.C., Pei, Z.J., Funkenbusch P.D., (2011). *Machining processes for sapphire wafers: a literature review*, Proceedings of the Institution of Mechanical Engineers, Part B: Journal of Engineering Manufacture, 225, 975-989.

13. Pawar, P., Ballav, R., Kumar, A., (2015). *An overview of machining process of alumina and alumina ceramic composites*, Manufacturing Science and Technology, 3(1), 10-15.
14. Pawar, P., Ballav, R., Kumar A., (2015). *Current scenario of machining process in advanced Al_2O_3 and Al_2O_3 ceramics composite materials: A study review*, Nonconventional Technologies Review, 19(4), 16-24.
15. Zhang, Y.N., Lin, B., Li, Z.C., (2013). *An overview of recent advances in chemical mechanical polishing (CMP) of sapphire substrates*, ECS Transactions, 52(1), 495-500.
16. Rogov, V.V., (2009). *Physicochemistry in Processes of the Formation of Functional Surfaces of Glass and Sapphire (α-Al_2O_3) Components for Electronics and Optical Systems in Tribochemical Polishing*, Journal of Superhard Materials, 31(4), 267-273.
17. Wen, D.H., Wan, Y.H., Hong, T., (2008). *Surface Integrity Induced by Abrasive Machining Sapphire Wafer*, Advanced Materials Research, 53-54, 311-316.
18. Shamir, A., Ishaaya, A.A., (2013). *Large volume ablation of Sapphire with ultra-short laser pulses*, Applied Surface Science, 270, 763-766.
19. Qi, L., Nishii, K., Yasui, M., Aoki H., Namba, Y., (2010). *Femtosecond laser ablation of sapphire on different crystallographic facet planes by single and multiple laser pulses irradiation*, Optics and Lasers in Engineering, 48, 1000-1007.
20. Wang, X.C., Lim, G.C., Zheng, H.Y., Ng, F.L., Liu, W., S.J. Chua, (2004). *Femtosecond pulse laser ablation of sapphire in ambient air*, Applied Surface Science, 228, 221-226.
21. Zheng, H.Y., Wang, X.C., (2009). *Some current research in femtosecond laser-induced surface ripple structures*, Int. J. Surface Science and Engineering, 3(1/2), 114-124.
22. Kim, K.S., Jones, D., Bente E., Girkin, J.M., Dawson, M.D., (2001). *Femtosecond laser micromachining of sapphire*, Lasers and Electro-Optics Society, LEOS 2001. The 14th Annual Meeting of the IEEE, 2, 762-763.
23. Rice, G., Jones, D., Kim, K.S., Girkin, J.M., Jarozynski, D., Dawson, M.D., (2003). *Micromachining of gallium nitride, sapphire and silicon carbide with ultrashort pulses*, *Proc. SPIE* 5147, ALT'02 International Conference on Advanced Laser Technologies, 299-307.
24. Yin, K., Duan, J., Sun, X., Wang, C., Luo Z., (2015). *Formation of superwetting surface with line-patterned nanostructure on sapphire induced by femtosecond laser*, Appl. Phys. A, 119(1), 69-74.
25. Chen, T.C., Darling, R.B., (2005). *Parametric studies on pulsed near ultraviolet frequency tripled Nd: YAG laser micromachining of sapphire and silicon*, Journal of Materials Processing Technology, 169, 214-218.
26. Chen T.C., Darling, R.B., (2008). *Laser micromachining of the materials using in microfluidics by high precision pulsed near and mid-ultraviolet Nd:YAG lasers*, Journal of Materials Processing Technology, 198, 248-253.
27. Han, J., Li, C., Zhang, M., Zuo, H., Meng, S., (2009). *An investigation of long pulsed laser induced damage in sapphire*, Optics & Laser Technology, 41, 339-344.
28. Lee, J.M., Jang, J.H., Yoo, T.K., (2000). *Scribing and cutting a blue LED wafer using a Q-switched Nd:YAG laser*, Appl. Phys. A, 70, 561-564.
29. Lee, J.M., Jang, J.H., Yoo, T.K., (2000). *Scribing blue LED wafer using laser-induced plasma-assisted ablation with a q-switched Nd:YAG laser*, Proceedings of SPIE Vol. 3933, 237-244.
30. Horisawa, H., Emura, H., Yasunaga N., (2004). *Surface machining characteristics of sapphire with fifth harmonic YAG laser pulses*, Vacuum, 73, 661-666.
31. Wyszynski, D., Skoczypiec, S., Furyk, K., (2012). *Mathematical Modelling of The Precise Laser Cutting Process of Al_2O_3 (Sapphire) Crystal*, Journal of Machine Enginering, 12(2), 20-28.
32. Tam, A.C., Brand, J.L., Cheng, D.C., Zapka, W., (1989). *Picosecond laser sputtering of sapphire at 266 nm*, Applied Physics Letters, 55(20), 2045-2047.
33. Tamhankar, A., Patel, R., (2011). *Optimization of UV laser scribing process for light emitting diode sapphire wafers*, Journal of Laser Applications, 23(3), 032001-1-032001-6.
34. Nebel, A., Herrmann, T., Henrich, B., Knappe, R., (2006). *Generation of tailored picosecond-pulse-trains for micro-machining*, Proc. of SPIE Vol., 6108, 610812-1-610812-8.
35. Zhou, Y., Wu, B., (2010). *Experimental study on infrared nanosecond laser-induced backside ablation of sapphire*, Journal of Manufacturing Processes, 12, 57-61.
36. Wortmann D., Gottmann, J., Brandt, N., Horn-Solle H., (2008). *Micro- and nanostructures inside sapphire by fs-laser irradiation and selective etching*, Optics Express, 16(3), 1517-1522.
37. Wei, X., Xie, X.Z., Hu W., Huang, J.F., (2012). *Polishing Sapphire Substrates by 355nm Ultraviolet Laser*, International Journal of Optics, 1-7.
38. Vilar, R., Sharma, S.P., Almeida, A., Cangueiro, L.T., Oliveira, V., (2014). *Surface morphology and phase transformations of femtosecond laser-processed sapphire*, Applied

Surface Science, 288, 313-323.
39. Chang, C.W., Chen, C.Y., Chang, T.L., Ting, C.J., Wang C.P., Chou, C.P., (2012). *Sapphire surface patterning using femtosecond laser micromachining*, Appl. Phys. A, 109, 441-448.
40. Wiesner, M., Ihlemann, J., (2011). *Fabrication of Sapphire Micro Optics by F_2-Laser Ablation*, Physics Procedia, 12, 239-244.
41. Bohme, R., Braun, A., Zimmer, K., (2002). *Backside etching of UV-transparent materials at the interface to liquids*, Applied Surface Science, 186, 276-281.
42. Kopitkovas, G., Lippert, T., David, C., Wokaun, A., Gobrecht, J., (2004). *Surface micromachining of UV transparent materials*, Thin Solid Films, 453-454, 31-35.
43. Gu, E., Jeon, C.W., Choi, H.W., Rice, G., Dawson, M.D., Illy, E.K., Knowles, M.R.H., (2004). *Micromachining and dicing of sapphire, gallium nitride and micro LED devices with UVcopper vapour laser*, Thin Solid Films, 453-454, 462-466.
44. Dai, Y., Xu, G., Cui, J., Bai, F., (2010). *Laser Micro-structuring of Sapphire Wafer and Fiber*, Proc. SPIE 7590, Micromachining and Microfabrication Process Technology XV, 75900O-1-75900O-8.
45. Liang, Z., Wang, X., Zhao, W., (2010). *A feasibility study on elliptical ultrasonic assisted grinding of sapphire substrate*, Int. J. Abrasive Technology, 3(3), 190-202.
46. Liang, Z., Wang, X., Wu, Y., Zhao, W., (2010). *Elliptical Ultrasonic Assisted Grinding (EUAG) of Monocrystal Sapphire - Surface Formation Characteristics -,* Advanced Materials Research, 126-128, 367-372.
47. Wu, Y., Liang, Z., Wang, X., Lin, W., (2010). *Elliptical Ultrasonic Assisted Grinding (EUAG) of Monocrystal Sapphire - Wear Behaviors of Resin Bond Diamond Wheel* -, Advanced Materials Research, 126-128, 573-578.
48. Liang, Z., Wang, X., Wu, Y., Xie, L., Liu, Z., Zhao, W., (2012). *An investigation on wear mechanism of resin-bonded diamond wheel in Elliptical Ultrasonic Assisted Grinding (EUAG) of monocrystal sapphire*, Journal of Materials Processing Technology, 212, 868-876.
49. Liang, Z., Wang, X., Wu, Y., Xie, L., Jiao, L., Zhao, W., (2013). *Experimental study on brittle–ductile transition in elliptical ultrasonic assisted grinding (EUAG) of monocrystal sapphire using single diamond abrasive grain*, International Journal of Machine Tools and Manufacture, 71, 41-51.
50. Wang, Q., Liang, Z., Wang, X., Zhao, W., Wu, Y., Jiao, L., Zhou, T., (2015). *Research on Surface Formation Mechanism In Elliptical Ultrasonic Assisted Grinding (EUAG) of Monocrystal Sapphire Using Structure Function Fractal Method*, Proceedings of the ASME 2015 International Manufacturing Science and Engineering Conference, 1, pp. V001T02A004; 5.
51. Yang, X.H., Han, J.C., Zhang, Y.M., Zuo, H.B., Zhang, X.J., (2006). *Research on Ultrasonic Vibration Grinding of the Hard and Brittle Materials*, Chinese Journal of Aeronautics, 19, S9-S13.
52. Liang, Z., Wu, Y., Wang, X., Peng, Y., Xu, W., Zhao, W., (2009). *A Two-dimensional Ultrasonically Assisted Grinding Technique for High Efficiency Machining of Sapphire Substrate*, Materials Science Forum, 626-627, 35-40.
53. Axinte, D., Butler-Smith, P., Akgun, C., Kolluru, K., (2013). *On the influence of single grit micro-geometry on grinding behavior of ductile and brittle materials*, International Journal of Machine Tools and Manufacture, 74, 12–18.
54. Wasmer, K., Pochon, P.M, Sage, D., Giovanola J.H., (2017). *Parametric experimental study and design of experiment modeling of sapphire grinding*, Journal of Cleaner Production, 141, 323-335.
55.Voloshin, A.V., Dolzhenkova, E.F., Litvinov, L.A., Petukhov, A.A., Slyunin, E.V., (2013). *The Influence of Coolant pH on Efficiency of Machining Sapphire*, Journal of Superhard Materials*,* 35(2), 126–130.
56.Gao, S., Kang, R.K., Dong, Z.G., Zhang, B., Wang Z.G., (2017). *Surface Integrity and Removal Mechanism in Grinding Sapphire Wafers with Novel Vitrified Bond Diamond Plates*, Materials and Manufacturing Processes, 32 (2), 121-126.
57. Cheng, J., Wu, J., Gong, Y.D., Wen, X.L. and Wen, Q., (2017). *Grinding forces in micro slot-grinding (MSG) of single crystal sapphire*, International Journal of Machine Tools and Manufacture, 112, 7-20.
58. Funkenbusch, P.D., Zhou, Y., Takahashi, T., Golini, D., (1998). *Grinding of single crystal sapphire: workpiece roughness correlations*, Wear, 218, 1-7.
59. Zhou, Y., Atwood, M., Golini, D., Smith, M., Funkenbusch, P.D., (1998). *Wear and self-sharpneing of vitrified bond diamond wheels during sapphire grinding*, Wear, 219, 42-25.
60. Funkenbusch, P.D., Takahashi, T., (1997). *Workpiece roughness and grindability*, SPIE Vol. 3134, 293-300.
61.Zhou, H., Xu, X., Zhuo, Z., Zang, Y., Xu, R.X., Feng, H., (2012). *Study on Improved Grinding Process of Sapphire with LED Substrate Material in Manufacturing Engineering*. Advanced Materials Research, 583, 314-317.
62. Bashe, J.R., Dempsey, G., Akwani, I.A.,

Jacoby, K.T., Hibbard, D.L., (2007). *Critical parameters for grinding large sapphire window panels*, Proc. SPIE 6545, Window and Dome Technologies and Materials X, 654517.

63. Han, P., Marinescu, I.D., Srivastava, A., (2009). *A Study on Electrolytic In-Process Dressing (ELId) Grinding of Sapphire With Acoustic Emission*, Proceedings of the ASME 2009 International Manufacturing Science and Engineering Conference, 1, 699-705.

64. Lei, H., Gu, Q., (2015). *Preparation of Cu-doped colloidal* SiO_2 *abrasives and their chemical mechanical polishing behavior on sapphire substrates*, Journal of Materials Science: Materials in Electronics, 26 (12), 10194-10200.

65. Lei, H., Tong, K., Wang, Z., (2016). *Preparation of Ce-doped colloidal* SiO_2 *composite abrasives and their chemical mechanical polishing behavior on sapphire substrates*, Materials Chemistry and Physics, 172, 26-31.

66. Zhang, Z., Yan, W., Zhang, L., Liu, W., Song, Z., (2011). *Effect of mechanical process parameters on friction behavior and material removal during sapphire chemical mechanical polishing*, Microelectronic Engineering, 88, 3020-3023.

67. Zhu, H., Tessaroto, L.A., Sabia, R., Greenhut, V.A., Smith, M., Niesz, D.E., (2004). *Chemical mechanical polishing (CMP) anisotropy in sapphire*, Applied Surface Science, 236, 120-130.

68. Park, C., Kim, H., Lee, S., Jeong, H., (2015). *The Influence of Abrasive Size on High-Pressure Chemical Mechanical Polishing of Sapphire Wafer*, International Journal of Precision Engineering and Manufacturing-Green Technology, 2(2), 157-162.

69. Aida, H., Doi, T., Takeda, H., Katakura, H., Kim, S.W., Koyama, K., Yamazaki, T., Uneda, M., (2012). *Ultraprecision CMP for sapphire, GaN, and SiC for advanced optoelectronics materials*, Current Applied Physics, 12, S41-S46.

70. Xu, W., Lu, X., Pan, G., Lei, Y., Luo, J., (2011). *Effects of the ultrasonic flexural vibration on the interaction between the abrasive particles; pad and sapphire substrate during chemical mechanical polishing (CMP)*, Applied Surface Science, 257, 2905-2911.

71. Xu, W., Lu, X., Pan, G., Lei, Y., Luo, J., (2010). *Ultrasonic flexural vibration assisted chemical mechanical polishing for sapphire substrate*, Applied Surface Science, 256, 3936-3940.

72. Xu L., Zou, C., Shi, X., Pan, G., Luo, G., Zhou, Y., (2015). *Fe-Nx/C assisted chemical–mechanical polishing for improving theremoval rate of sapphire*, Applied Surface Science, 343, 115-120.

73. Bastawros, A.F., Chandra, A., Poosarla, P.A., (2015). *Atmospheric pressure plasma enabled polishing of single crystal sapphire*, CIRP Annals - Manufacturing Technology, 64(1), 515-518.

74. Xu, Y., Lu, J., Xu X., (2015). *The Research of Reactivity betweenNano-abrasives and Sapphire during Polishing Process*, Integrated Ferroelectrics: An International Journal, 159(1), 41-48.

75. Zhu, H., Niesz, D.E., Greenhut, V.A., (2005). *The effect of abrasive hardness on the chemical-assisted polishing of (0001) plane sapphire*, J. Mater. Res., 20(2), 504-520.

76. Rogov, V.V., Rublev, N.D., Krotenko, T.L., Troyan, A.V., (2008). *A Study of Intensity of Tribochemical Contact Interaction Between a Polishing Compound and Sapphire in Machining*, Journal of Superhard Materials, 30(4), 273–275.

77. Hu, G.X., Hu, X.D., Jin, Y.F., Hu, X.Z., Li, W., (2006). *The Development of the Precise Double Sided Polishing Machine*, Key Engineering Materials, 315-316, 375-379.

78. Kumar, P., More, S., Singh, R., Joshi S.S., (2013). *Experimental characterization of plane and conformal hydrodynamic polishing of machined single crystal sapphire*, Manufacturing Letters, 1, 70-73.

79. Askinazi, J., Hasan, W., Dunn, D., La Fleur, L.D., (1997). *Computer controlled fabrication of sapphire windows*, SPIE Vol. 3134, 301-306.

80. Kim, H.M., Park, G.H., Seo, Y.G., Moon, D.J., Cho, B.J., Park. J.G., (2015). *Comparison between sapphire lapping processes using 2-body and 3-body modes as a function of diamond abrasive size*, Wear, 332-333, 794-799.

81. Gagliardi, J.J., Kim, D., Soko, J.J., Zazzera, L.A., Romero, V.D., Atkinson, M.R., Nabulsi, F., Zhang H., (2013), *A case for 2-body material removal in prime LED sapphire substrate lapping and polishing*, Journal of Manufacturing Processes, 15, 348-354.

82. Kim, H.M., Manivannan, R., Moon, D.J., Xiong, H., Park, J.G., (2013). *Evaluation of double sided lapping using a fixed abrasive pad for sapphire substrates*, Wear, 302(1), 1340-1344.

83. Zhang K., Wen, D., Yuan J., (2009). *Study on the Abrasive Effecting Factors of the Removal Rate during Dual-Lapping Sapphire Wafer*, Key Engineering Materials, 407-408, 550-554.

84. Lin, Z.C., Hsu, Y.C., (2012). *A calculating method for the fewest cutting passes on sapphire substrate at a certain depth using specific down force energy with an AFM probe*, Journal of Materials Processing Technology, 212, 2321-2331.

85. Huang, J.C., Weng, Y.J., (2014). *The Study on the Nanomachining Property and Cutting Model of Single-Crystal Sapphire by Atomic Force Microscopy*, SCANNING, 36, 599-607.

86.Schinker, M.G., (1991). Subsurface damage

mechanisms at high-speed ductile machining of optical glasses, Precision Engineering, 13(3), 208-218.
87. Wang, J., Feng, P., Zhang, J., Zhang, C., Pei, Z., (2016). *Modeling the dependency of edge chipping size on the material properties and cutting force for rotary ultrasonic drilling of brittle materials*, International Journal of Machine Tools and Manufacture, 101, 18-27.
88. Matsumaru, K., Takata, A., Ishizaki, K., (2005). *Advanced thin dicing blade for sapphire substrate*, Science and Technology of Advanced Materials, 6, 120-122.
89. Hu, X., Song, Z., Pan, Z., Liu, W., Wu, L., (2009). *Planarization machining of sapphire wafers with boron carbide and colloidal silica as abrasives*, Applied Surface Science, 255, 8230–8234.
90. Wu, S.J., Hsu, H.C., Lin, W.F., (2016). *Reduction of Residual Stresses in Sapphire Cover Glass Induced by Mechanical Polishing and Laser Chamfering Through Etching*, Advances in Technology Innovation, 1(2), 29-32.
91. Li, T., Visvanathan, K., Gianchandani, Y.B., (2013). *A batch-mode micromachining process for spherical structures*, J. Micromech. Microeng., 24(2), 025002 (8pp).
92. Rogov, V.V., Tkach, V.N., Rublev, N.D., Troyan, A.V., Popel'nyuk, V.N., (2008). *A Study of Surface Condition of Sapphire (α-Al_2O_3) Workpieces upon Their Finishing Operation*, Journal of Superhard Materials, 30(3), 192–197.
93. Mohammadi, H., Patten, J.A., (2016). *Anisotropy Effect on Cutting Monocrystal Sapphire By Micro-Laser Assisted Machining Technique*, ASME 2016 11th International Manufacturing Science and Engineering Conference, 1, pp. V001T02A018; 7.
94. Zhang C., Feng, P., Zhang, J., (2013). *Ultrasonic vibration-assisted scratch-induced characteristics of C-plane sapphire with a spherical indenter*, International Journal of Machine Tools and Manufacture, 64, 38-48.
95. Lee, H., Kasuga, H., Ohmori, H., Lee, H., Jeong, H., (2011). *Application of electrolytic in-process dressing (ELID) grinding and chemical mechanical polishing (CMP) process for emerging hard–brittle materials used in light-emitting diodes*, Journal of Crystal Growth, 326, 140-146.
96. Muttamara, A., Fukuzawa, Y., Mohri, N., Tani, T., (2004). *Effects of Structural Orientation on EDM Properties of Sapphire*, Materials Transactions, 45(7), 2486-2488.
97. Ho, K.H., Newman, S.T., (2003). *State of the art electrical discharge machining (EDM)*, International Journal of Machine Tools & Manufacture, 43, 1287-1300.

Received: December 15, 2016 / Accepted: June 10, 2017 / Paper available online: June 20, 2017 © International Journal of Modern Manufacturing Technologies.